

Design study for an airborne multi-wavelength, multi-depolarization HSRL

Ilya Serikov

Max Planck Institute for Meteorology



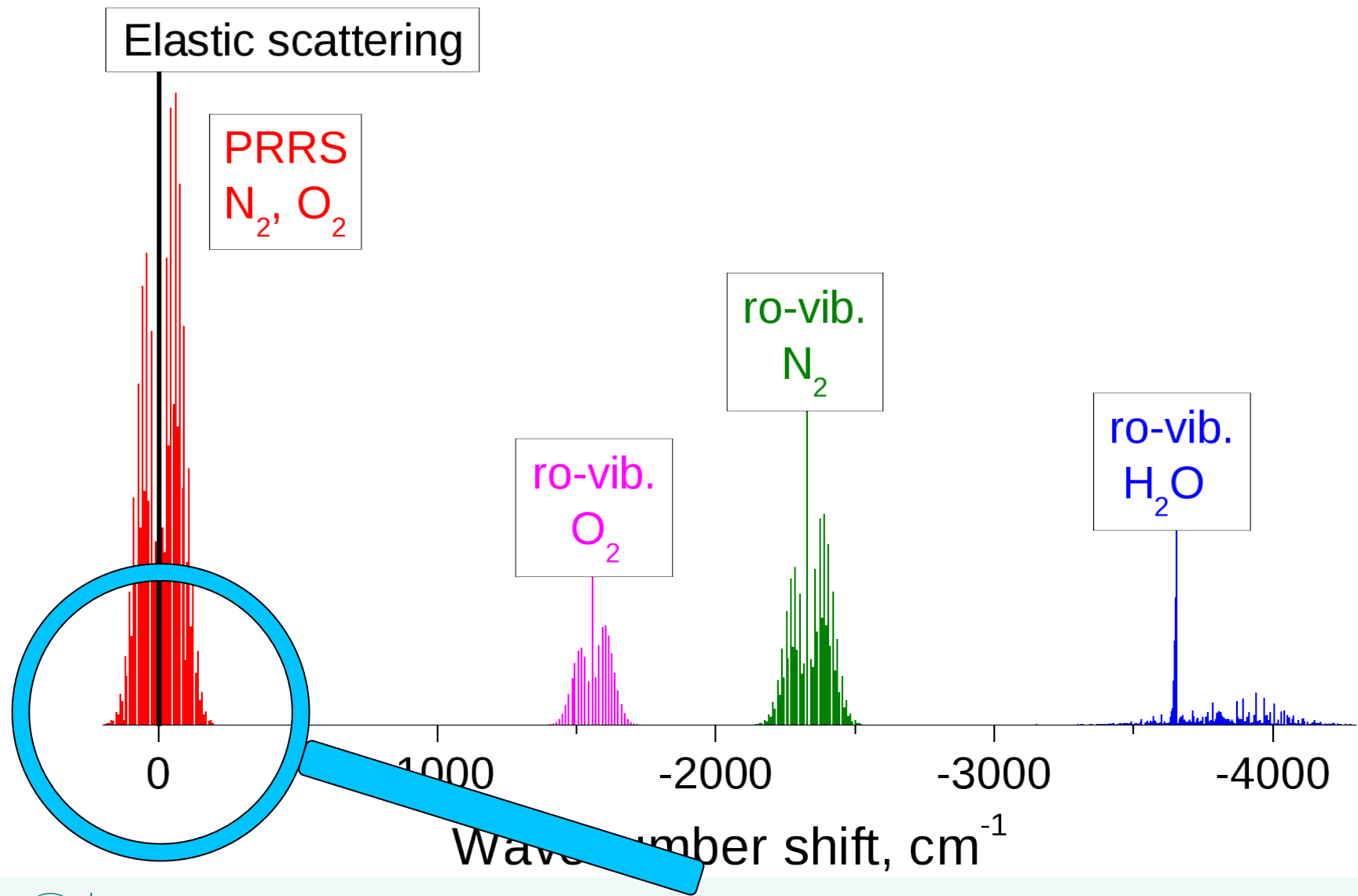
Max-Planck-Institut
für Meteorologie

Outline

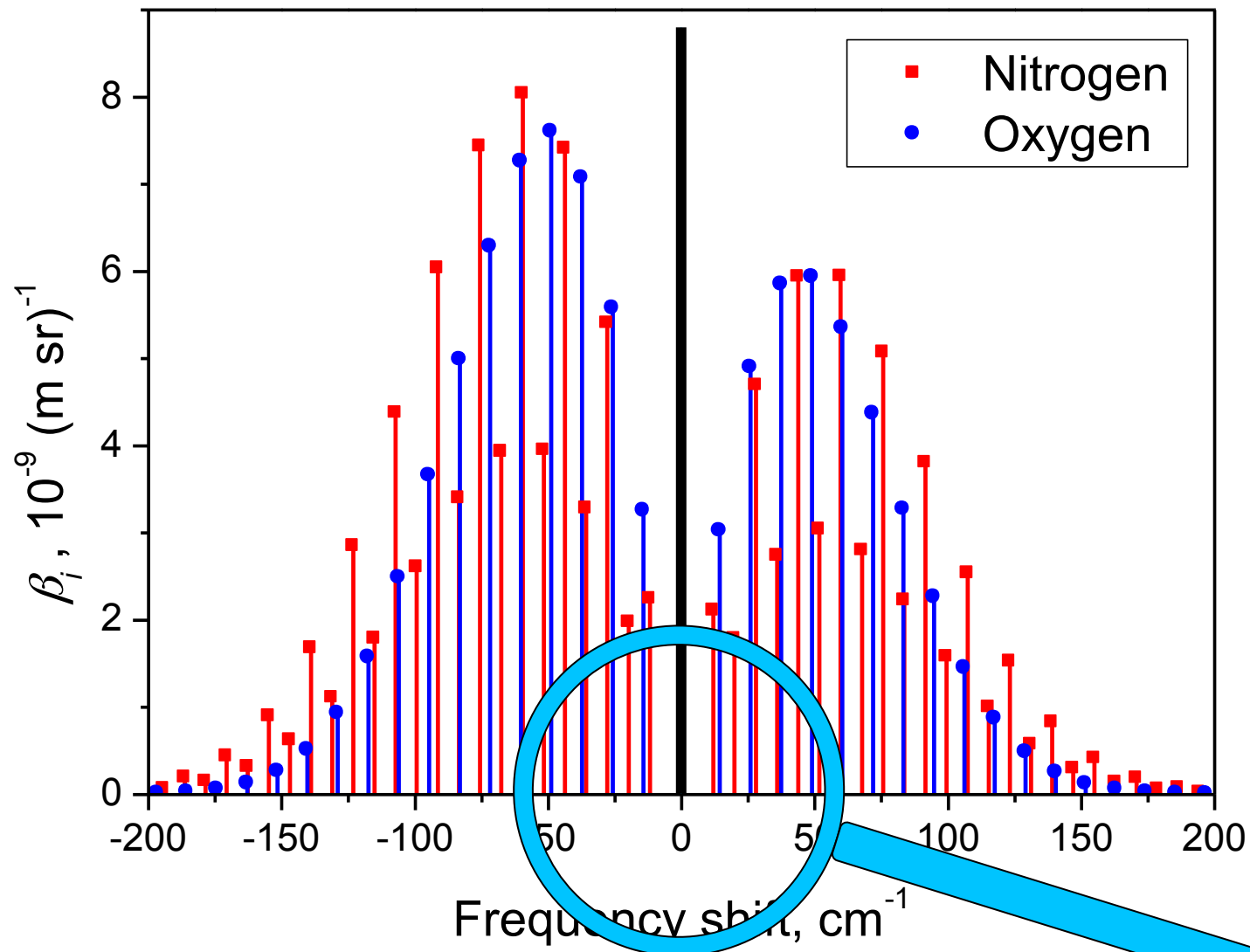
- HSRL task and the cross-talk suppression required
- Fabry-Pérot Interferometer (FPI) for HSRL channel
 - The concept
 - FPI parameters in the scope of application
 - Filtering efficiency expected
 - Stability issues



Atmospheric response to laser pumping

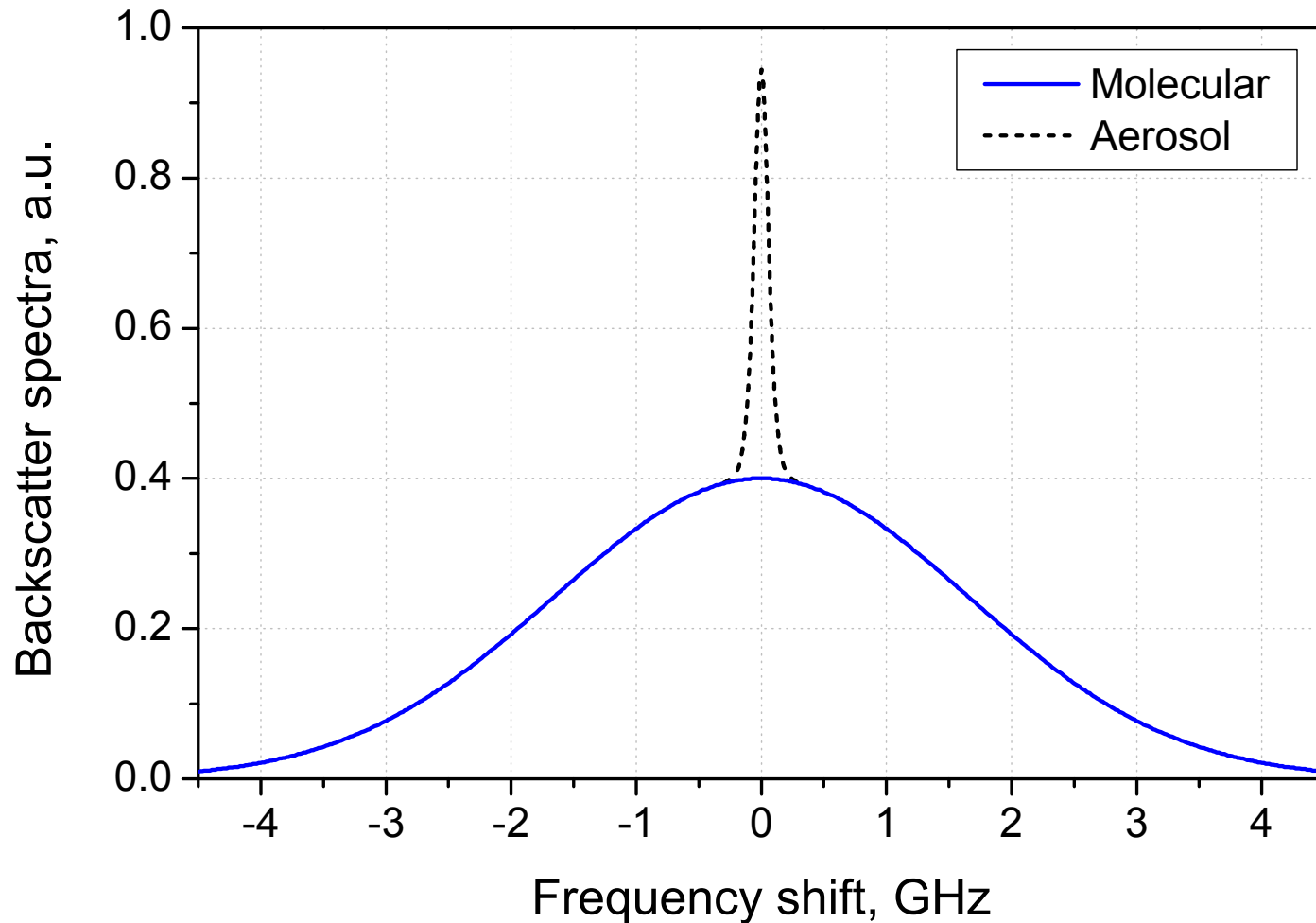


Pure rotational Raman spectra of N₂ and O₂



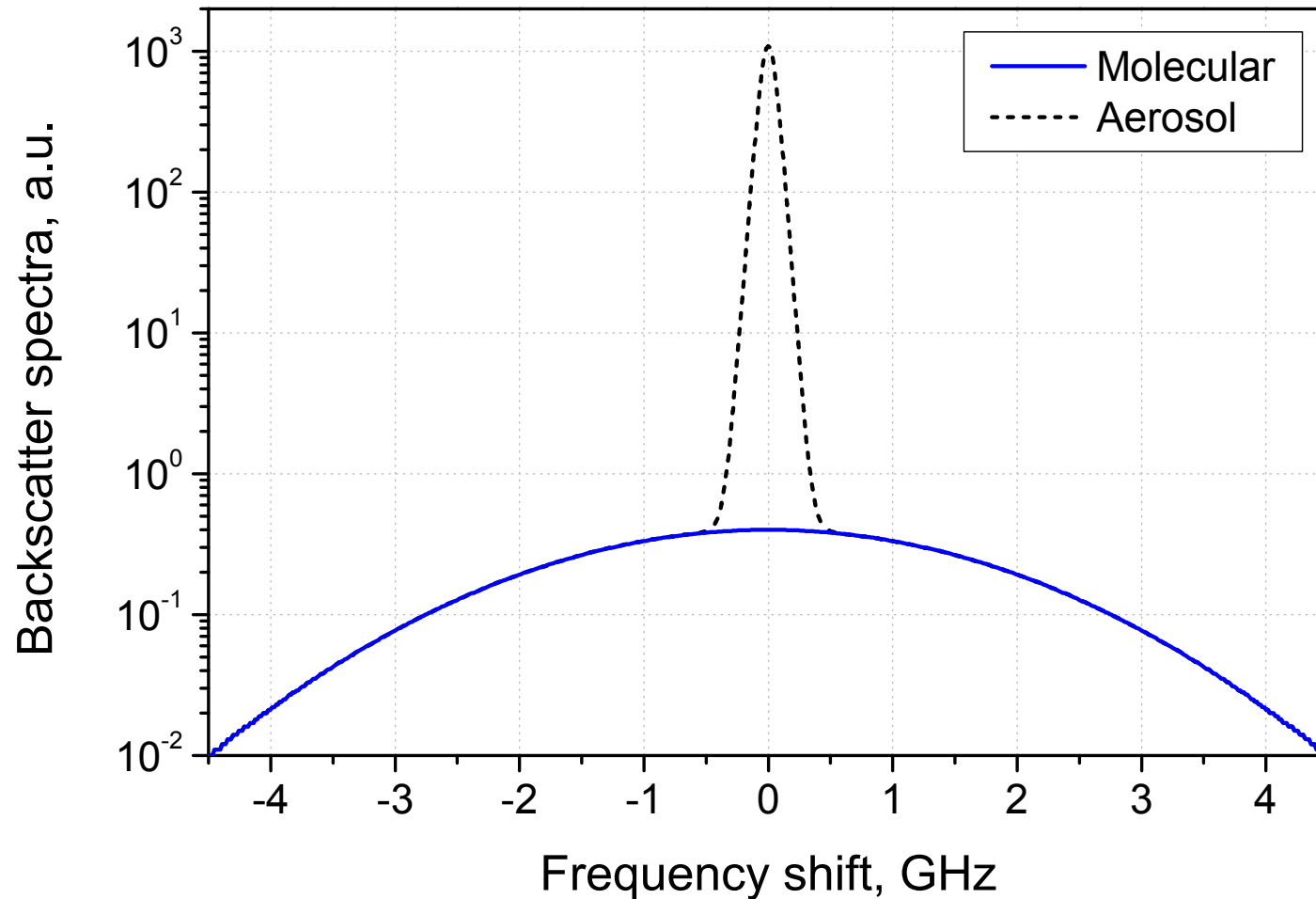
Example for air mixture at 1 atm and 273 K. Excitation at 355 nm.

Molecular and aerosol elastic scattering



Scattering ratio **1.05**, $\lambda = 355$ nm, $T = 300$ K

Molecular and aerosol elastic scattering



Scattering ratio **100**, $\lambda = 355$ nm, $T = 300$ K

Scattering ratio in clouds

	355 nm	532 nm	1064 nm
Ice cloud @ 10km $\beta_{\pi} = 0.2$ /km/sr	80	370	6,200
Droplet cloud @ 5km $\beta_{\pi} = 0.8$ /km/sr	180	880	14,600

Suppression required

$S = M + K \cdot A$ ← signal in molecular channel

M molecular scattering; A aerosol scattering; K cross-talk

$k = K \pm \delta k$ ← estimated cross-talk

$m = S - k \cdot A$ ← estimated molecular signal

$m = M \pm \delta k \cdot A$

$\frac{\delta k}{K} \leq \frac{1}{K} \cdot \frac{m - M}{M} / \frac{A}{M}$ ← cross-talk estimation accuracy

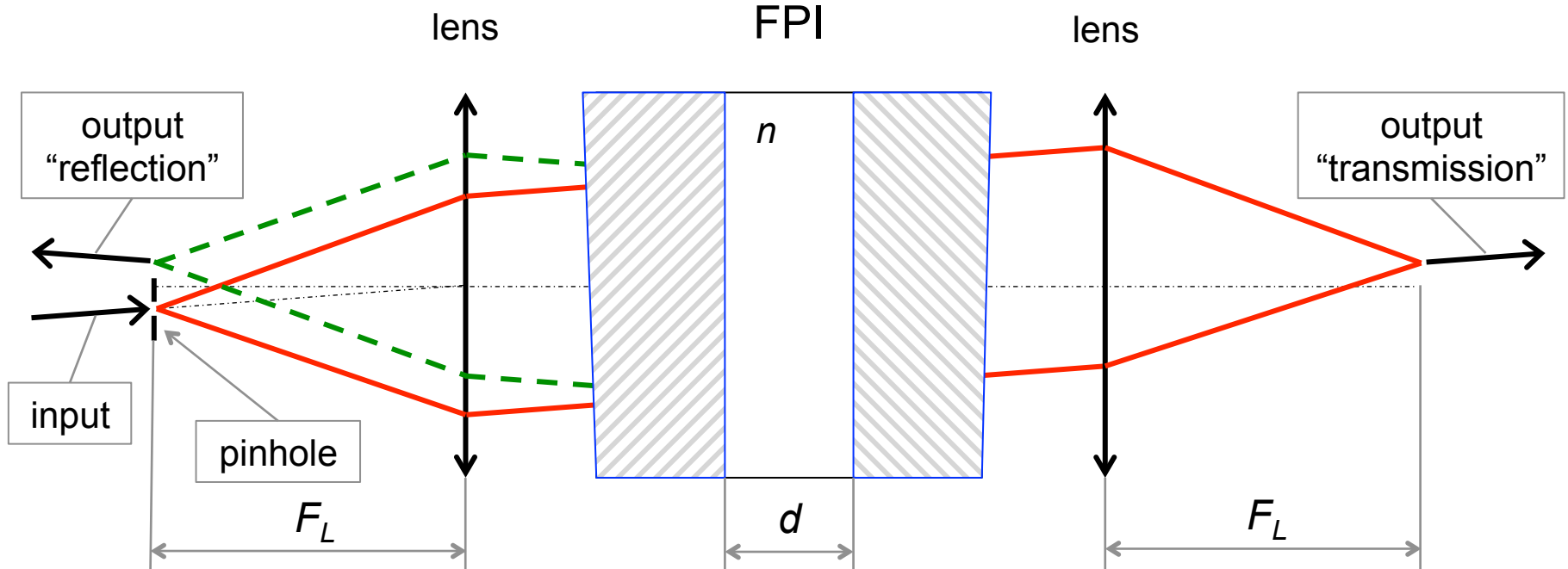
A/M	$\Delta k / K$ ($\delta m / M = 1\%$)		
	$K = 10^{-1}$	$K = 10^{-2}$	$K = 10^{-3}$
10	1%	10%	–
100	0.1%	1%	10%
1000	0.01%	0.1%	1%

The concept logic:

1. **Fabry-Pérot Interferometers** as HSRL filter at 355nm
(possibly also at 532nm and 1064nm)
2. **Iodine filtering technique** at 532nm (alternative to interferometers)
3. **Narrow field-of-view** receiving telescopes
(to low the beam divergence on interferometer)
4. **Beam expansion** (to fit to the receiving field-of-view)
5. **Low laser pulse energy** (to conform the eye-safety requirements)
6. **High pulse repetition rate** (to increase the number of photons emitted)
7. **Fiber optics** decoupling telescope and interferometers
(for better mechanical stability)
8. **Extra telescopes for depolarization** channel
(multimode fibers do not maintain polarization)
9. **Extra “near”-range telescope**
(to extend the range for extinction measurement)



Fabry-Pérot Interferometer (FPI)



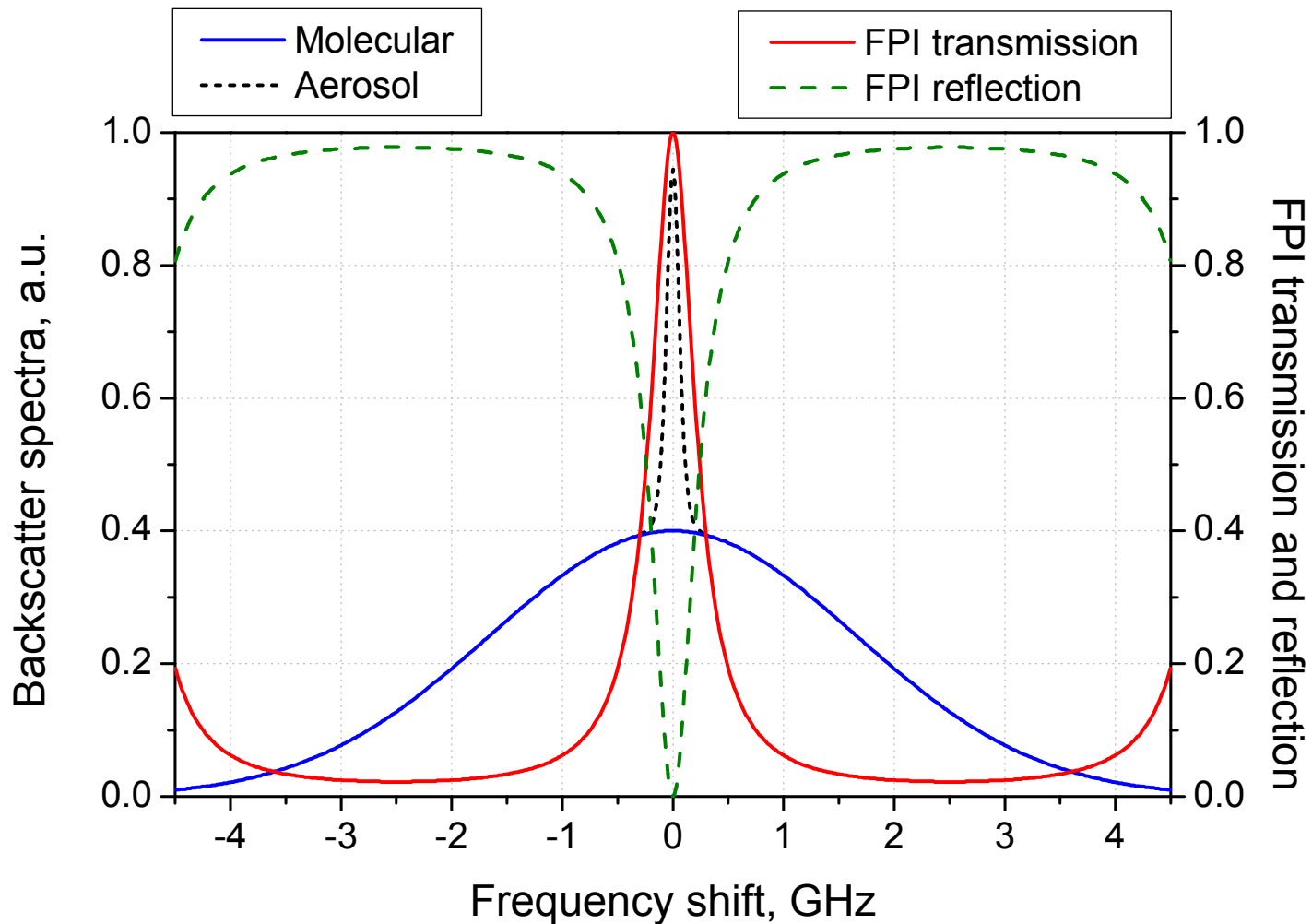
Transmission and reflection

$$f_T = \frac{1}{1 + \frac{4R}{(1-R)^2} \sin^2(2\pi\nu nd \cos \theta)} \quad f_R = 1 - f_T$$

Phase matching criterion:

$$2\pi\nu nd \cos \theta = \pi k, k \in N$$

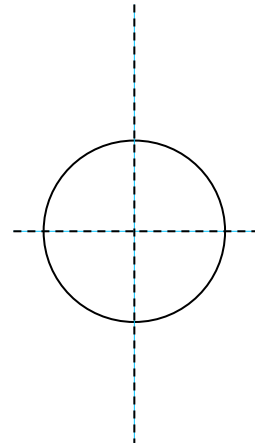
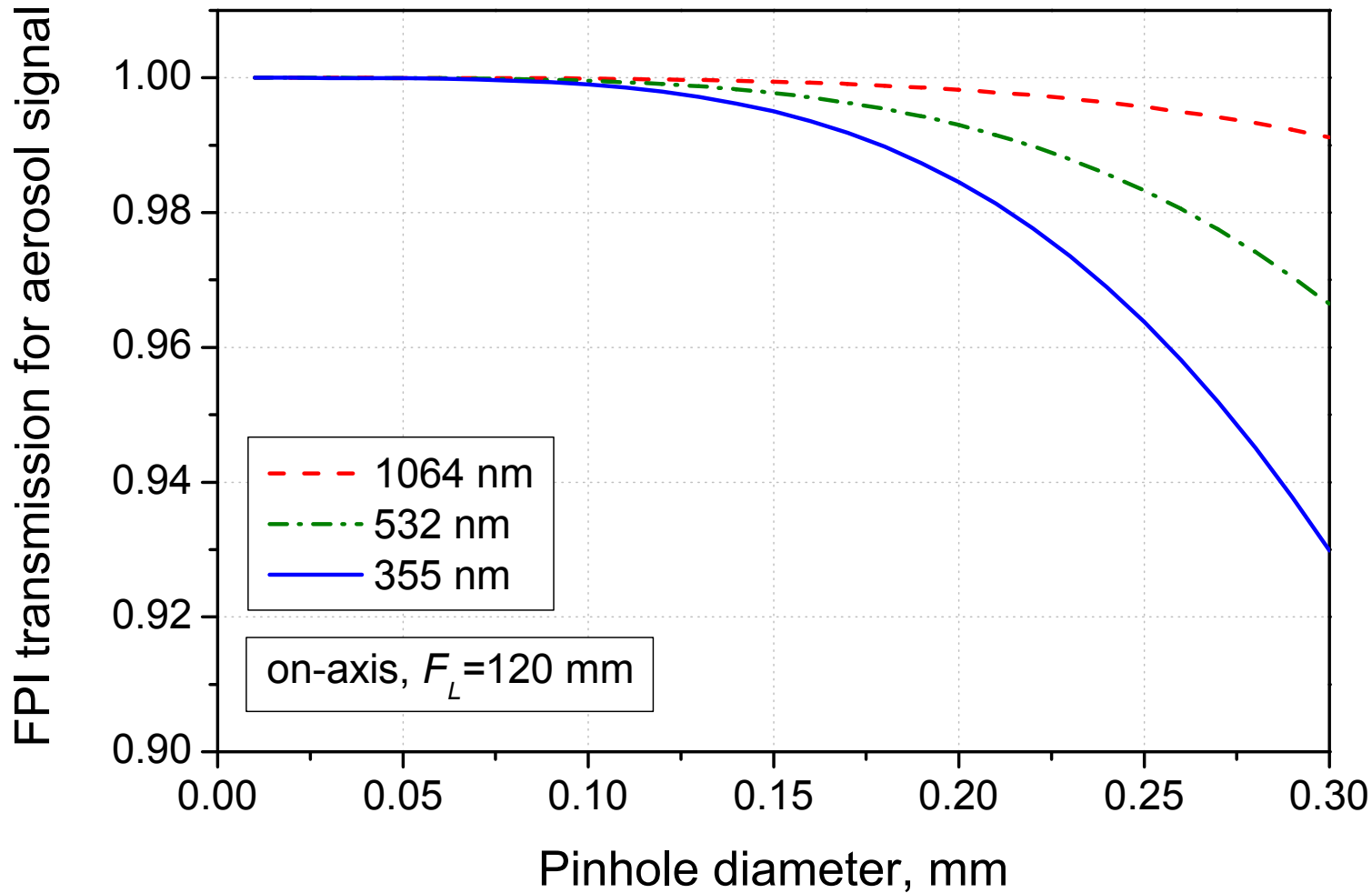
Interferometer tuning concept



Phase matching criterion:

$$2\pi(m \cdot \nu_0)nd \cos \theta = m \cdot \pi k, k \in N$$

Transmission for axial divergent beam

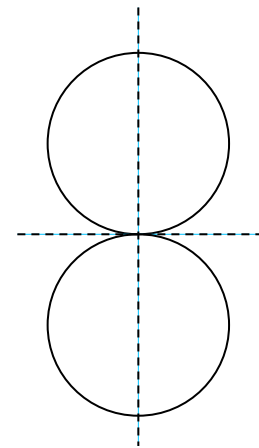
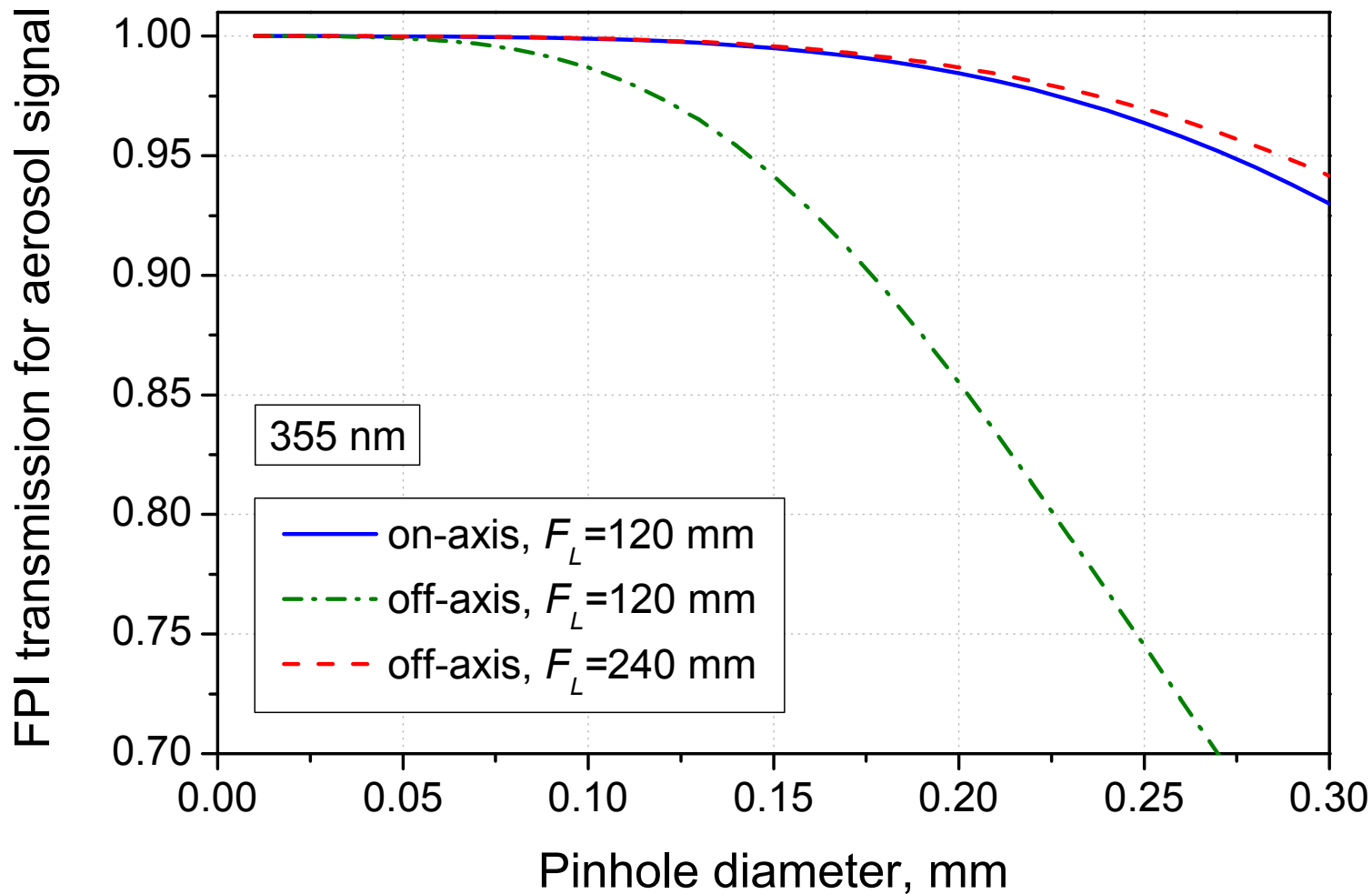


$$f_T = \frac{1}{1 + \frac{4R}{(1-R)^2} \sin^2(2\pi vnd \cos \theta)}$$

$$F_L = 120 \text{ mm}; R = 0.44; d = 30 \text{ mm}; n = 1$$

Transmission for off-axial divergent beam

355 nm

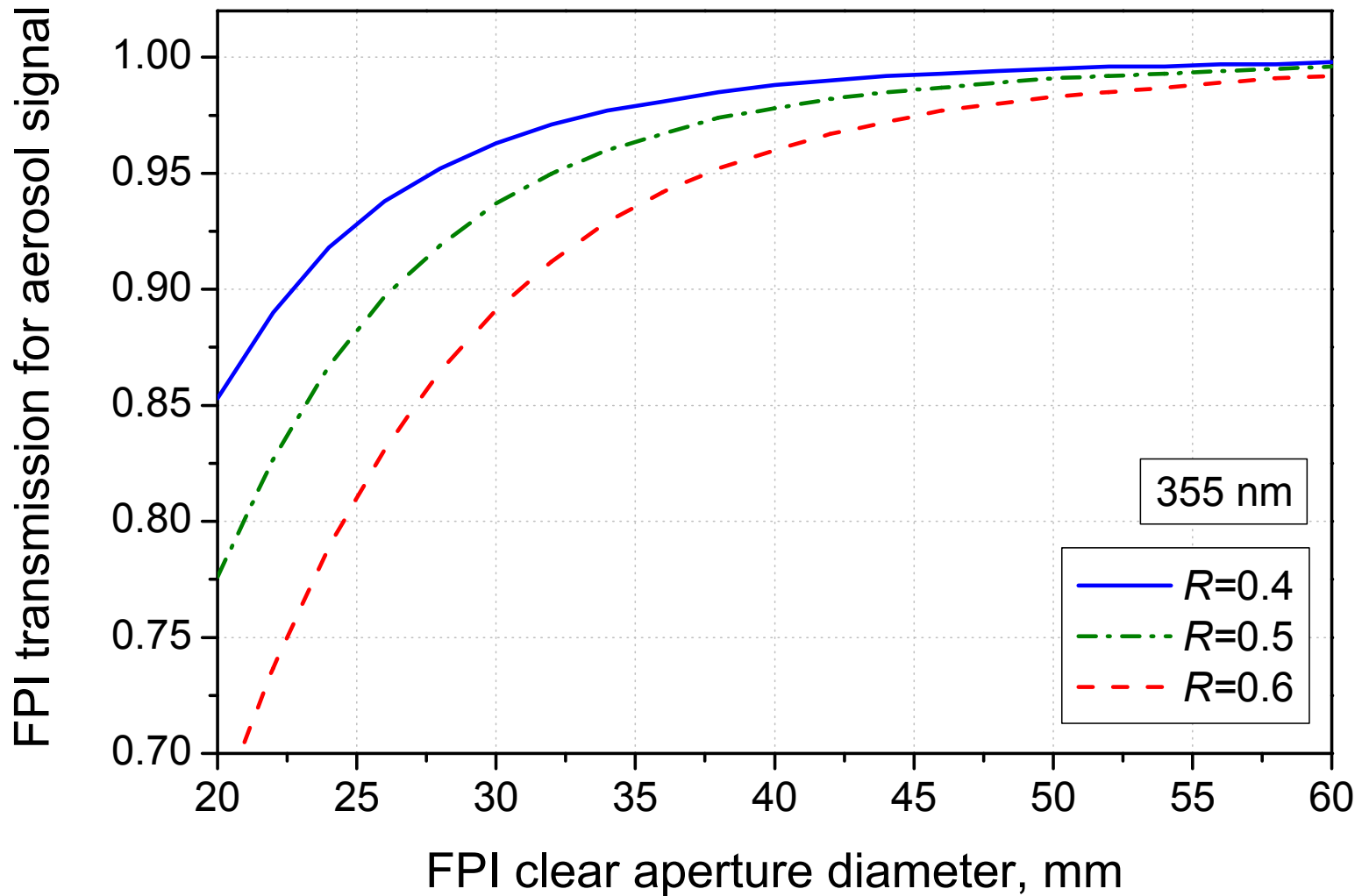


For off-axis configuration the pinhole is displaced from axis by pinhole radius

$$R = 0.44; d = 30 \text{ mm}; n = 1$$

Clear aperture impact

355 nm

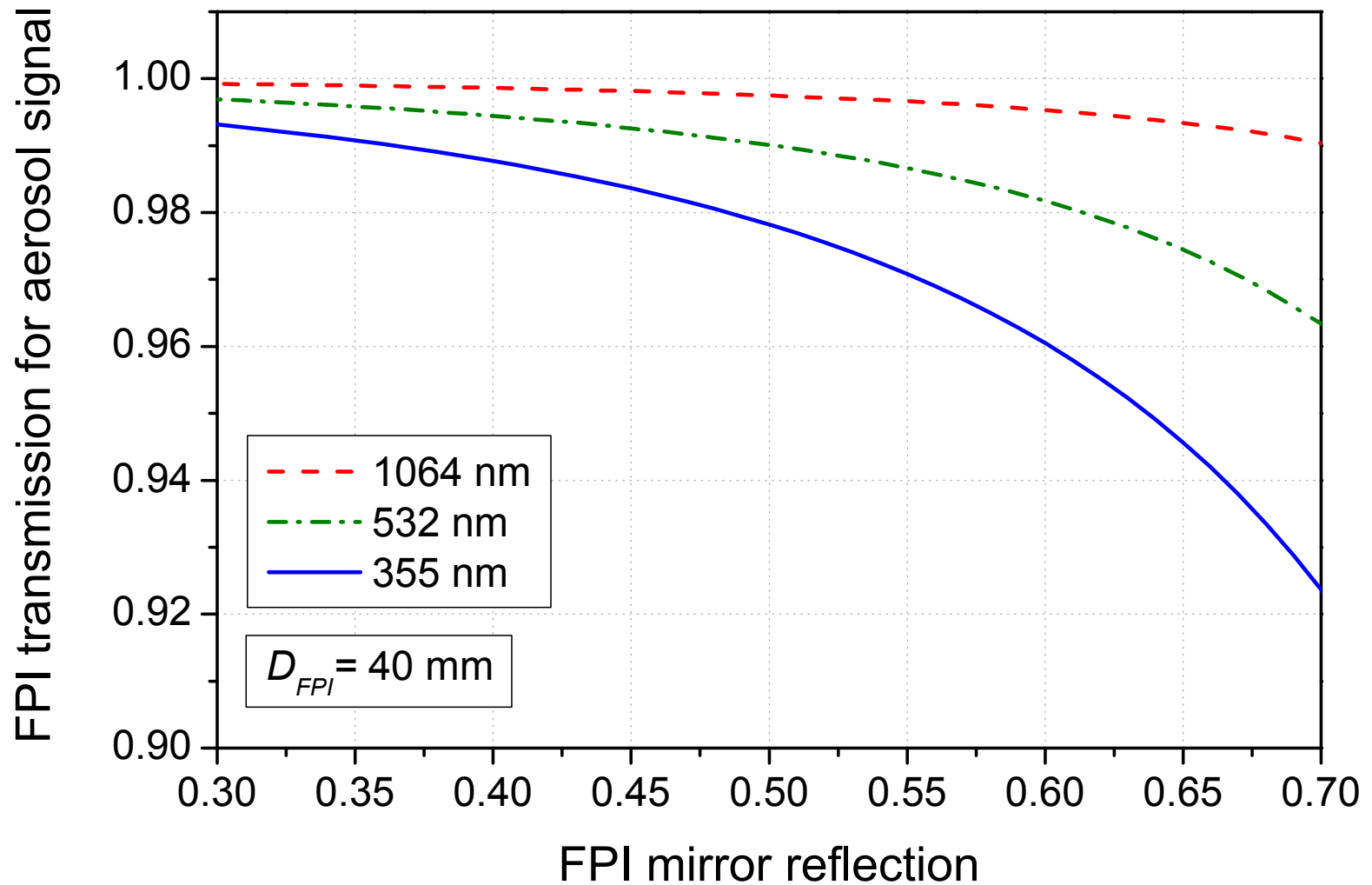


$$d_p / f_{\#} = \text{const}$$

$$d_p = 0.2 \text{ mm}; F_L / D_{CA} = 3$$

$$d = 30 \text{ mm}; n = 1$$

Impact of mirror reflection coefficient



$d = 30$ mm

$d_p = 0.2$ mm; $F_L = 120$ mm; $D_{FPI} = 40$ mm; $n = 1$



Effect of mirror roughness

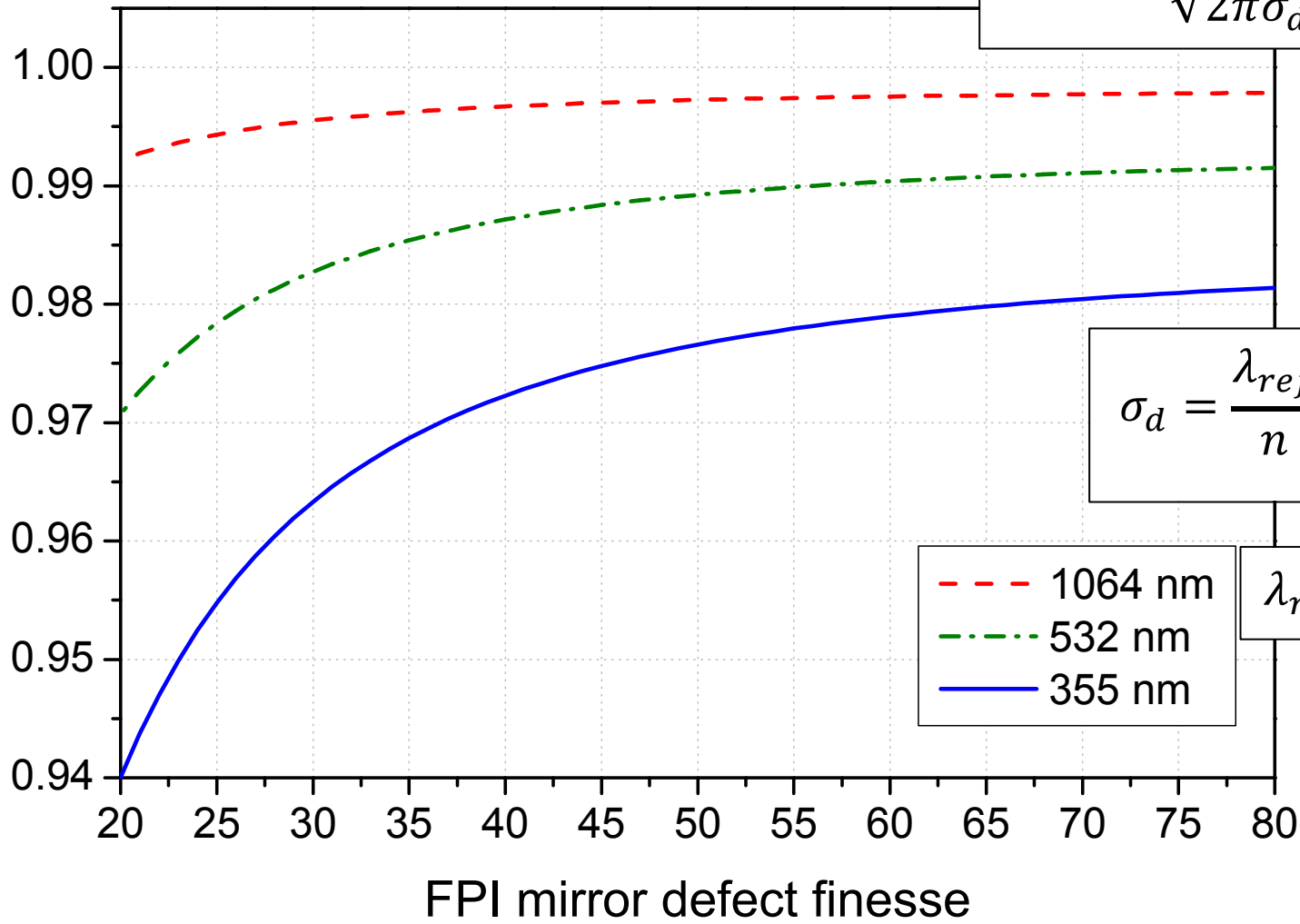
FPI transmission for aerosol signal

$$\rho(\delta) = \frac{1}{\sqrt{2\pi}\sigma_d} \exp\left(-\frac{\delta^2}{2\sigma_d^2}\right)$$

$$\sigma_d = \frac{\lambda_{ref}}{n} \frac{1}{4\sqrt{2 \ln 2} F_d}$$

$$\lambda_{ref} = 532 \text{ nm}$$

- - - 1064 nm
- · - · 532 nm
- 355 nm

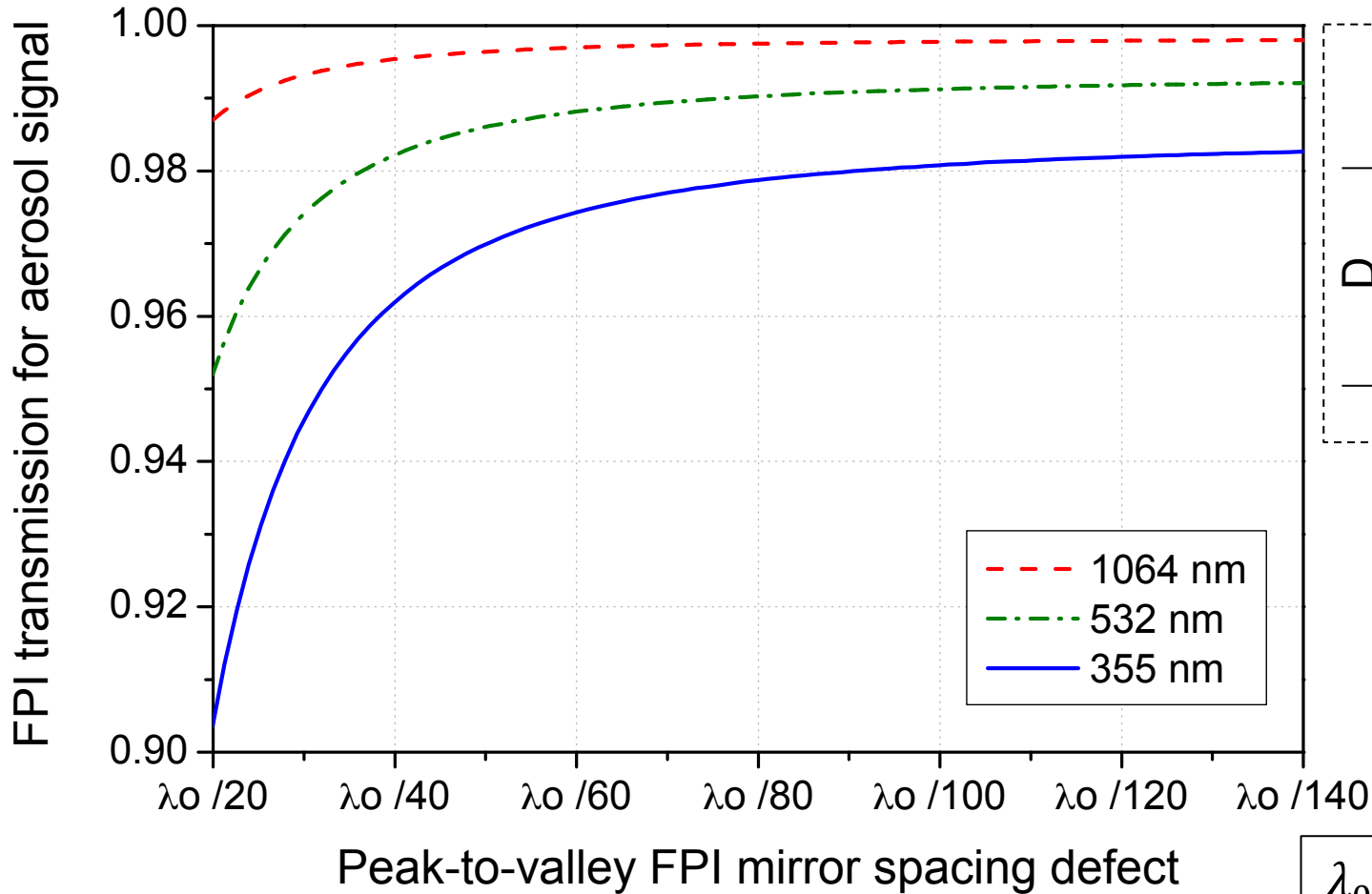


$R = 0.44; d = 30 \text{ mm}$

$d_p = 0.2 \text{ mm}; F_L = 120 \text{ mm}; D_{FPI} = 40 \text{ mm}; n = 1$

Effect of mirror sphericity

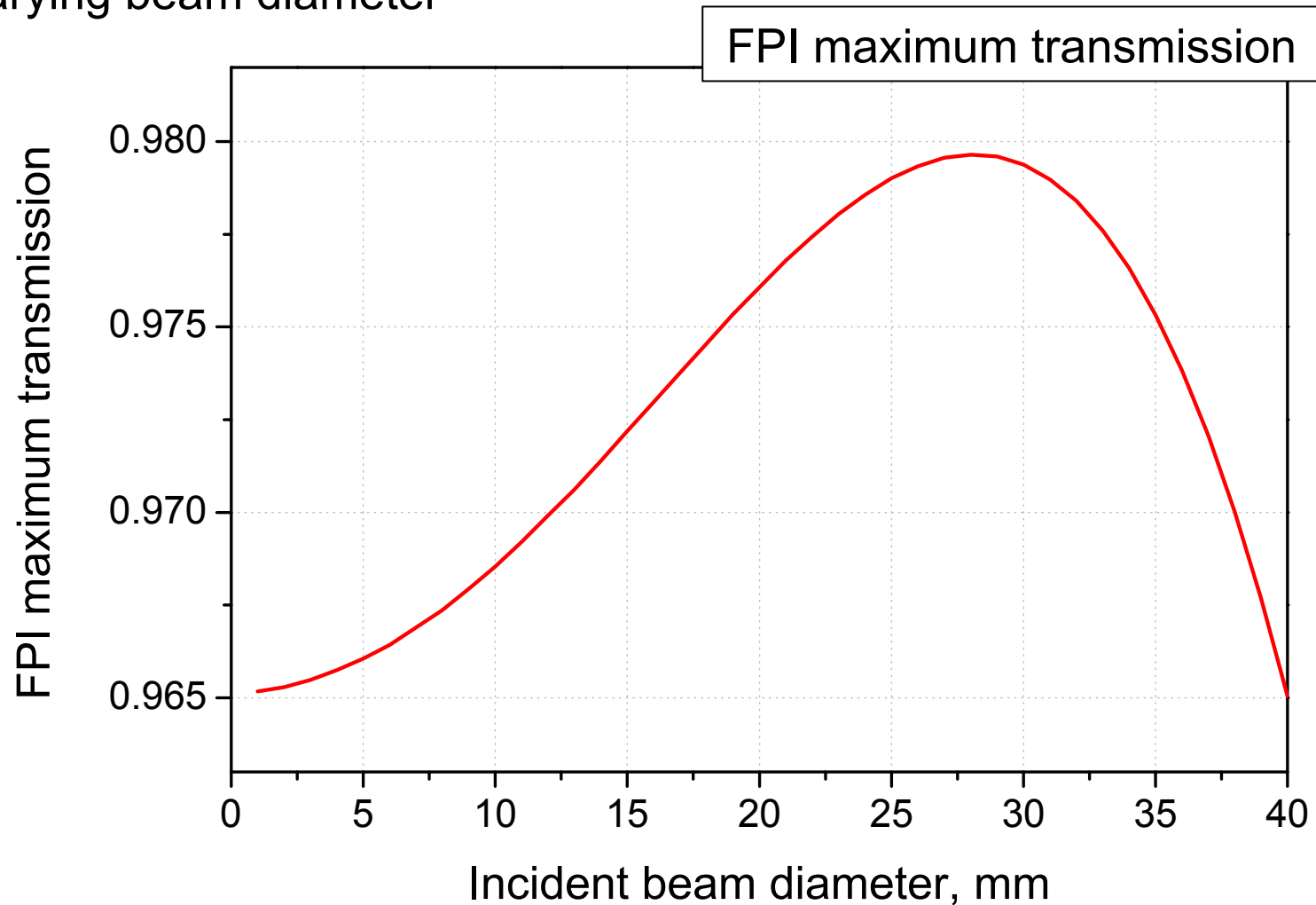
(a) constant beam diameter, clear aperture completely filled



*mirror flatness $\lambda/100$; $R = 0.44$; $d = 30 \text{ mm}$
 $d_p = 0.2 \text{ mm}$; $F_L = 120 \text{ mm}$; $D_{FPI} = 40 \text{ mm}$; $n = 1$*

Effect of mirror sphericity

(b) varying beam diameter



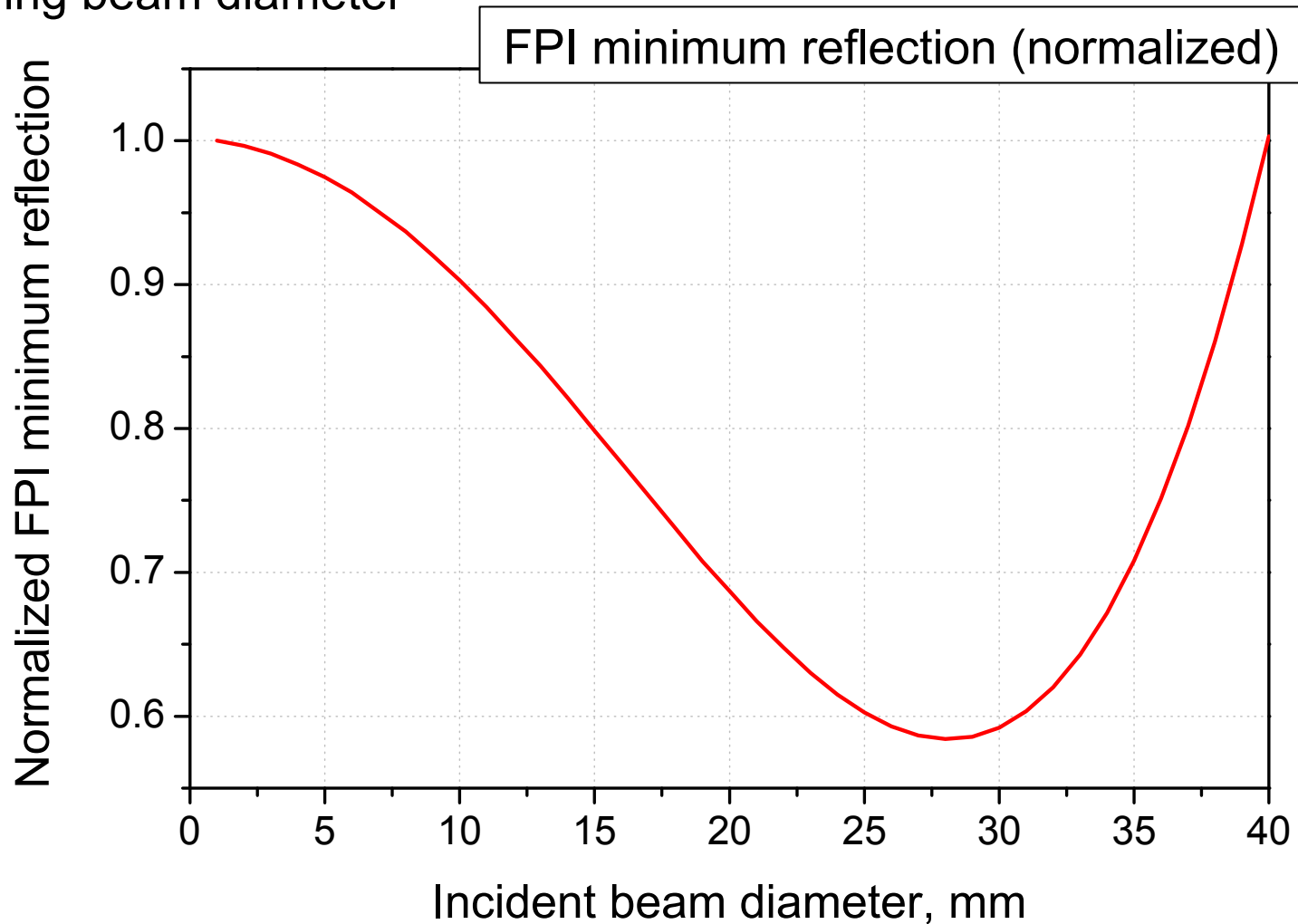
mirror flatness $\lambda/100$; $R = 0.44$; $d = 30$ mm

$d_p = 0.2$ mm; $F_L = 120$ mm; $D_{FPI} = 40$ mm; $n = 1$



Effect of mirror sphericity

(b) varying beam diameter

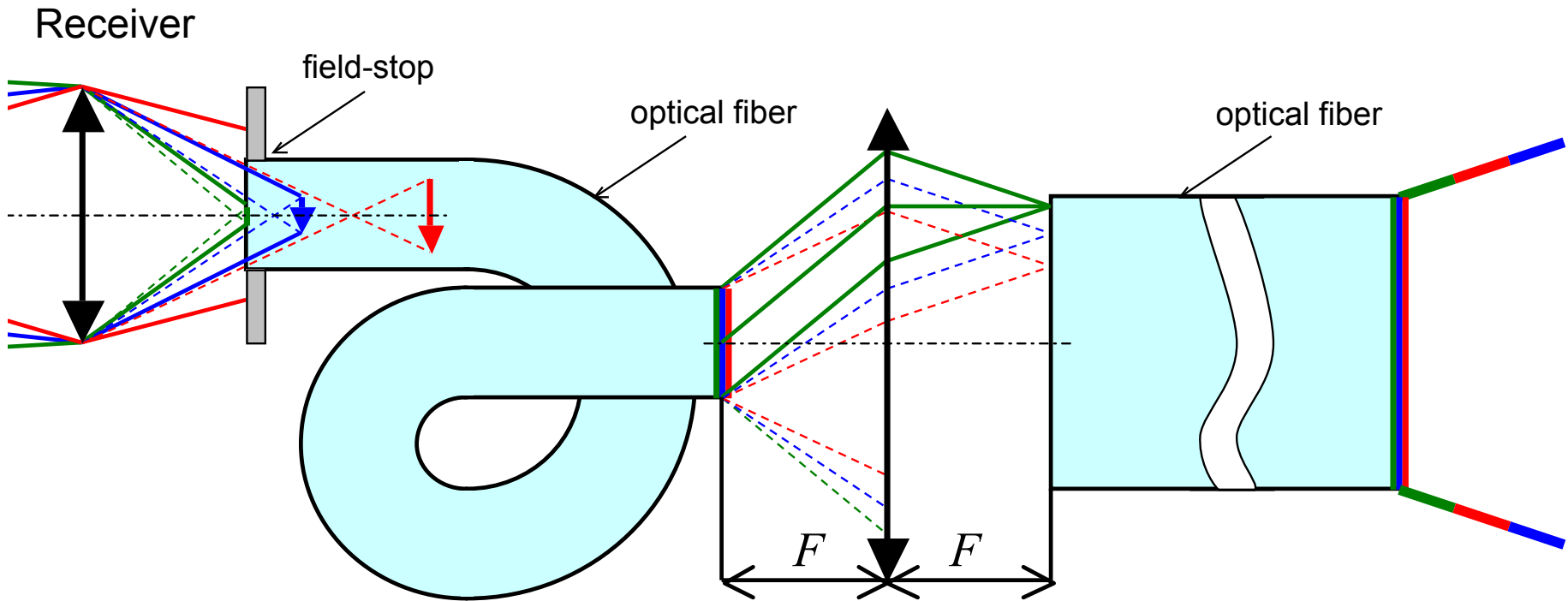


mirror flatness $\lambda/100$; $R = 0.44$; $d = 30$ mm

$d_p = 0.2$ mm; $F_L = 120$ mm; $D_{FPI} = 40$ mm; $n = 1$



“Fiber-lens-fiber” optical scrambler



- input fiber scrambles the beam across the fiber aperture
- lens translates the beam angle into the focusing point position
- output fiber scrambles the beam across the fiber aperture

Filtering efficiency

Reflection efficiency for molecular signal

$$Q_m^{[N]} = \int_{-\infty}^{+\infty} I_m(f - f_0)(1 - f_T(f))^N df$$

Reflection efficiency for aerosol signal

$$Q_a^{[N]} = \int_{-\infty}^{+\infty} I_L(f - f_0)(1 - f_T(f))^N df$$

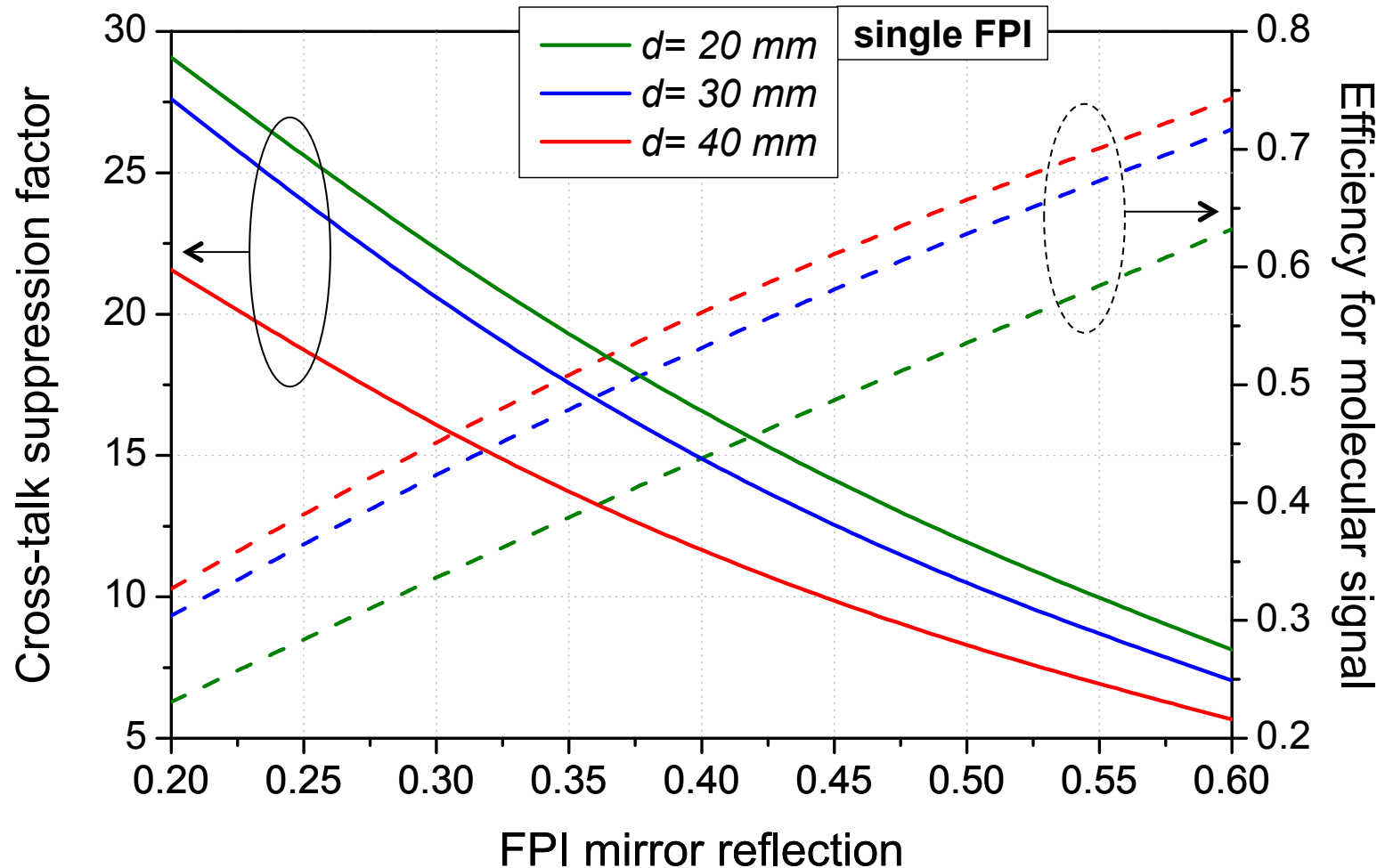
Cross-talk suppression factor

$$K^{[N]} = \frac{Q_m^{[N]}}{Q_a^{[N]}}$$

N – number of sequential FPI filtering cascades

Filtering efficiency, 1xFPI

355 nm

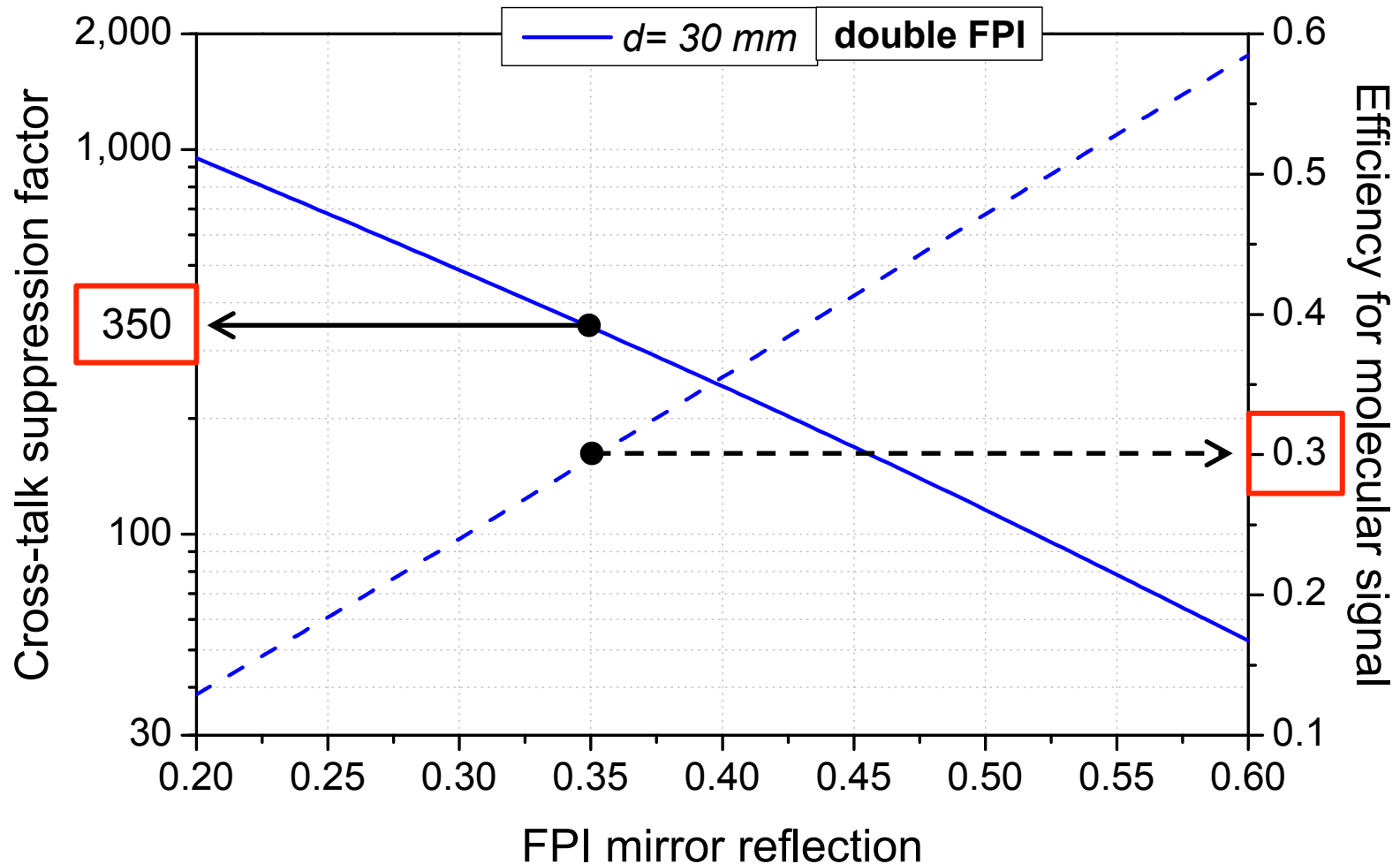


$$\Delta f_{355} = 135 \text{ MHz}$$

$$d_p = 0.2 \text{ mm}; F_L = 120 \text{ mm}; D_{FPI} = 40 \text{ mm}; F_d = 30; n = 1$$

Filtering efficiency, 2xFPI

355 nm

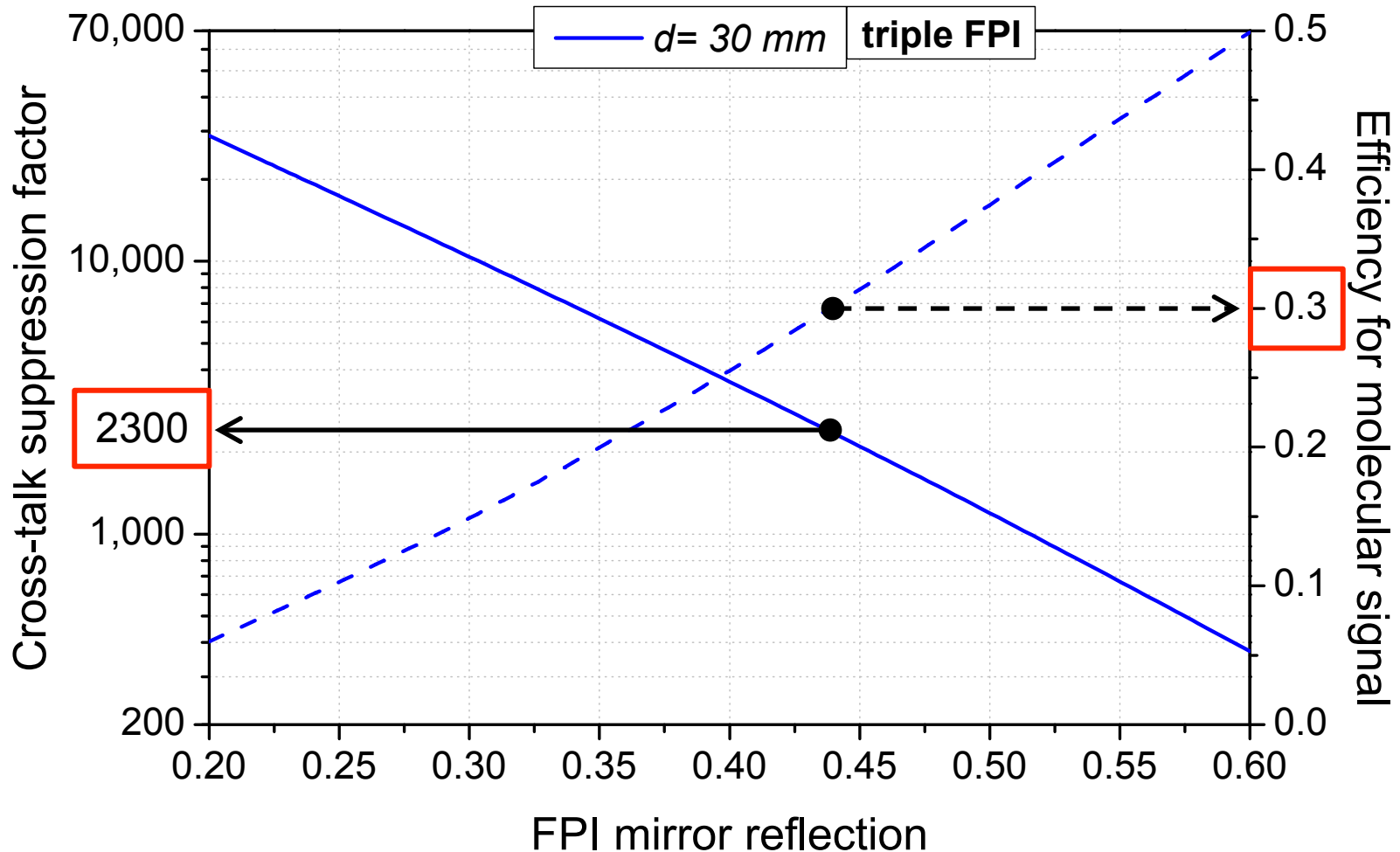


$$\Delta f_{355} = 135 \text{ MHz}; d = 30 \text{ mm}$$

$$d_p = 0.2 \text{ mm}; F_L = 120 \text{ mm}; D_{FPI} = 40 \text{ mm}; F_d = 30; n = 1$$

Filtering efficiency, 3xFPI

355 nm



$$\Delta f_{355} = 135 \text{ MHz}; d = 30 \text{ mm}$$

$$d_p = 0.2 \text{ mm}; F_L = 120 \text{ mm}; D_{FPI} = 40 \text{ mm}; F_d = 30; n = 1$$

Filtering efficiency, summary

A. Reflection coefficient optimized for UV

# FPI	355 nm			532 nm			1064 nm		
	R	Suppr.	Eff., %	R	Suppr.	Eff., %	R	Suppr.	Eff., %
1	0.2	28	30	0.2	46	23	0.2	80	10
2	0.35	350		0.35	1140	22	0.35	5900	7
3	0.44	2300		0.44	14500	22	0.44	$2.4 \cdot 10^5$	7

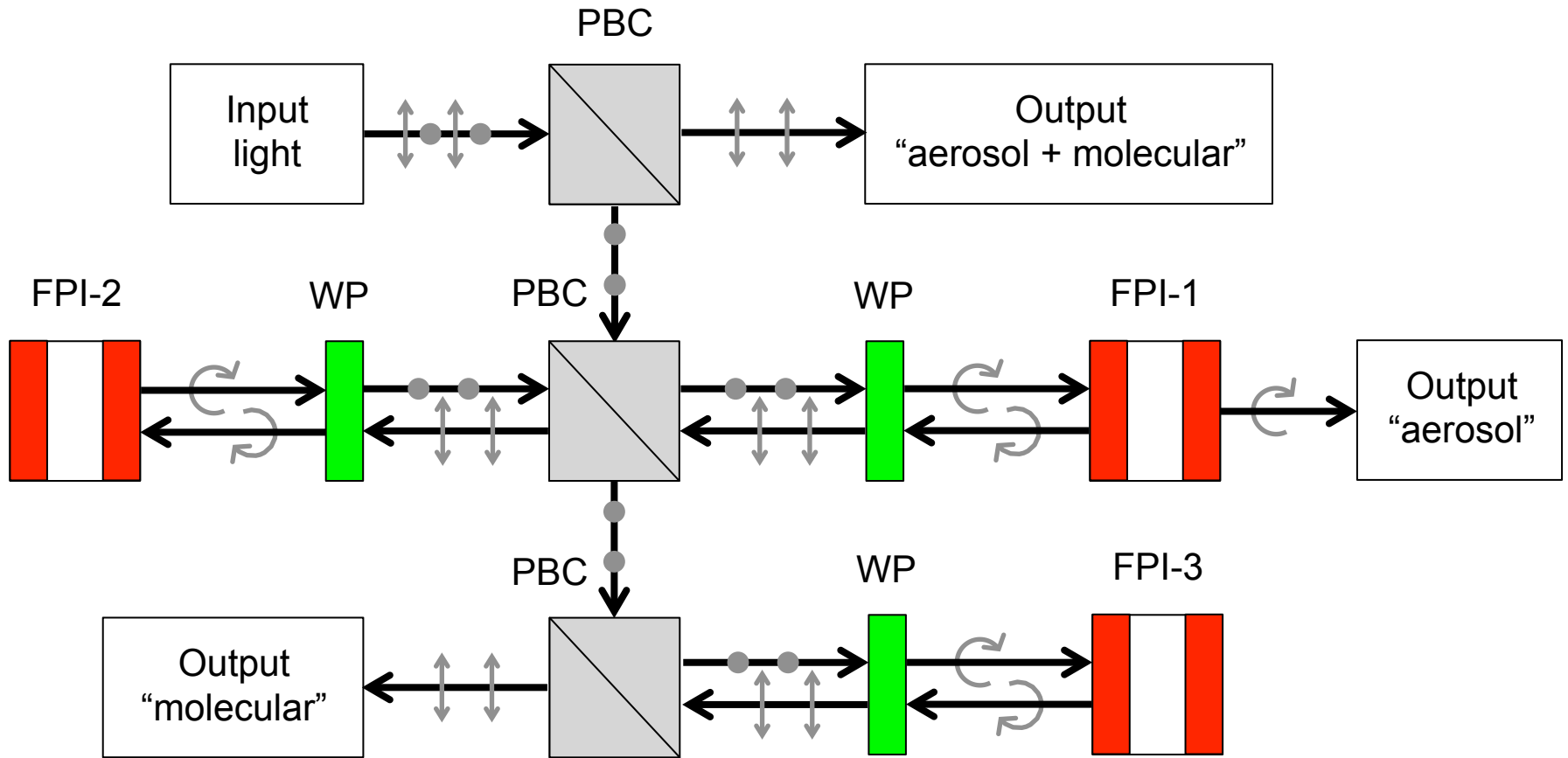
B. Reflection coefficient optimized for each wavelength

# FPI	355 nm			532 nm			1064 nm		
	R	Suppr.	Eff., %	R	Suppr.	Eff., %	R	Suppr.	Eff., %
1	0.2	28	30	0.26	39	30	0.47	45	30
2	0.35	350		0.43	650		0.63	850	
3	0.44	2300		0.52	5600		0.7	8300	

C. Scattering ratio in clouds

	80÷180	370÷880	6,200÷14,600
--	--------	---------	--------------

Polarization-sensitive decoupling



PBC – Polarizing Beam splitting Cubes; WP – quarter-Wave Plates

Stability

Phase matching criterion

$$\frac{2\pi}{c} f \cdot n \cdot d \cdot \cos \theta = \pi k, k \in N$$

a) Frequency, (f)

- laser frequency instability,
- Doppler shift

$$f_0 \pm \Delta f$$

- due to axial wind,
- due to aircraft pitch-angle bias,

$$f_0 \pm 2 f_0 V / c$$

$$f_0 \pm 2 f_0 V_A \sin(\phi) / c$$

b) Effective mirror spacing, ($n \cdot d$)

- thermal expansion of spacers,
- temperature of air in the mirror gap,
- pressure of air in the mirror gap,

$$d_0 \pm d_0 \cdot CTE \cdot T$$

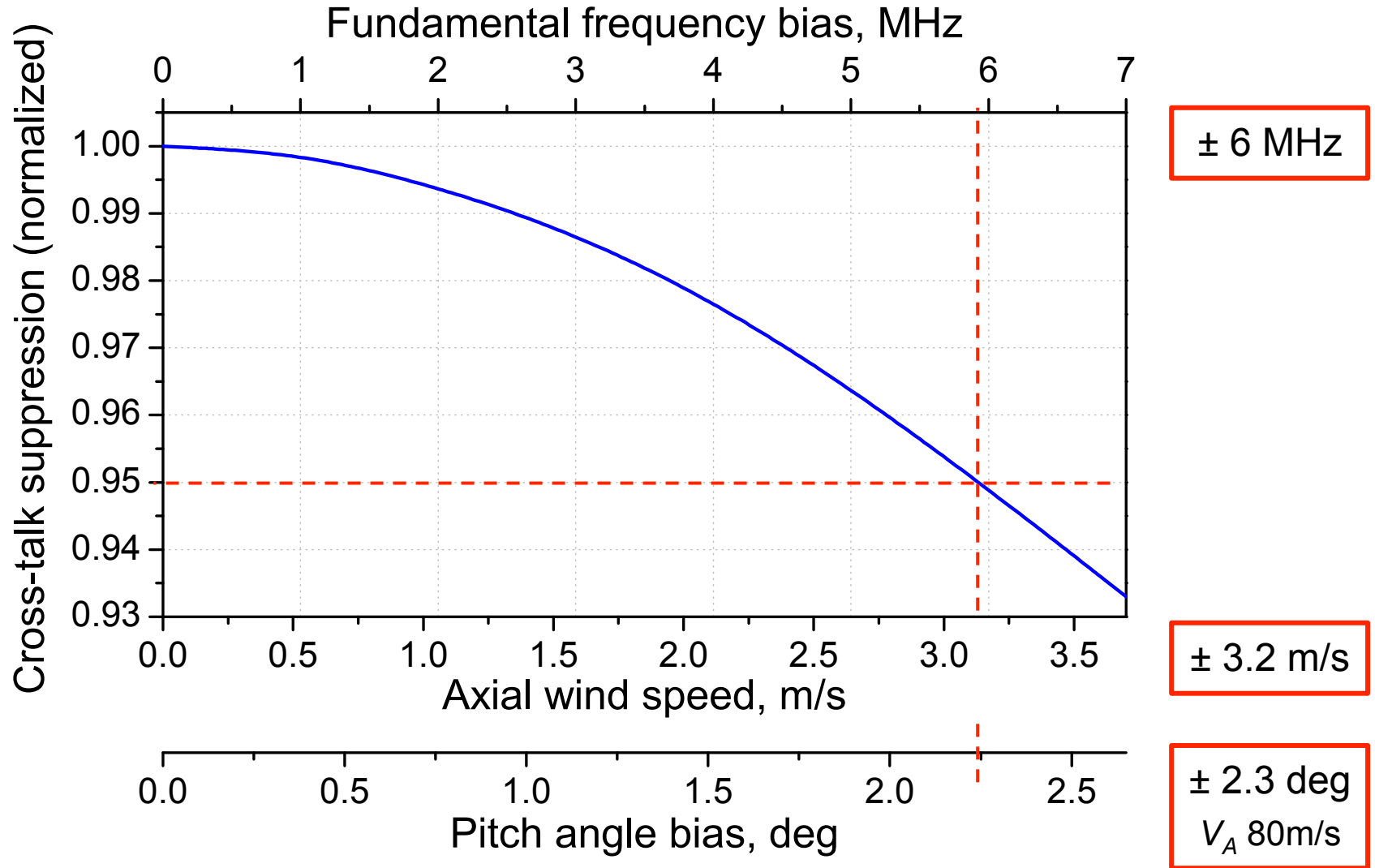
$$\delta n \sim 1 / T$$

$$\delta n \sim P$$

c) Incident angle, (θ)

Sensitivity to frequency bias

3xFPI, 355 nm



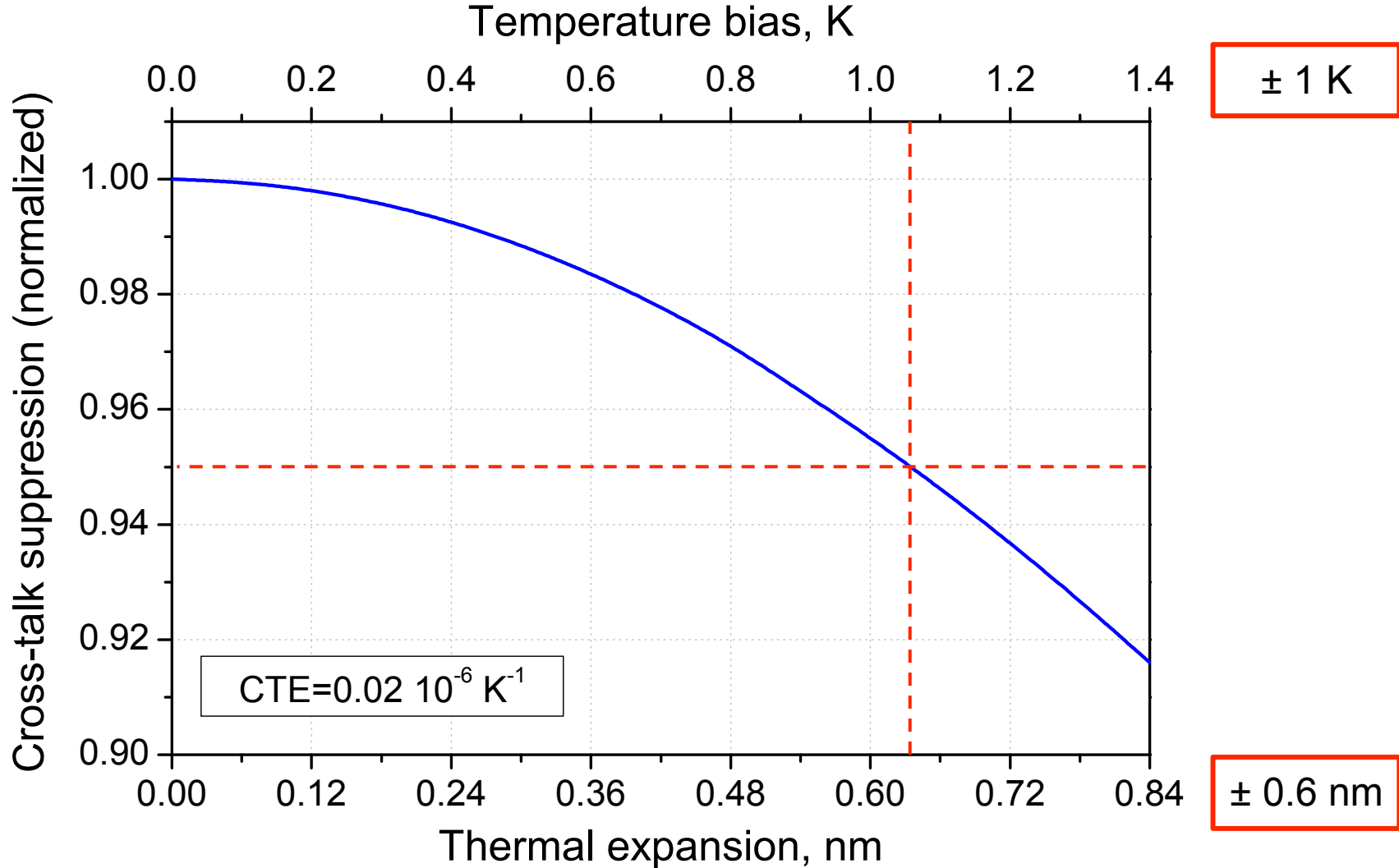
$$\Delta f_{355} = 135 \text{ MHz}; R = 0.44; d = 30 \text{ mm}$$

$$d_p = 0.2 \text{ mm}; F_L = 120 \text{ mm}; D_{FPI} = 40 \text{ mm}; F_d = 30; n = 1$$



Thermal expansion impact

3xFPI, 355 nm



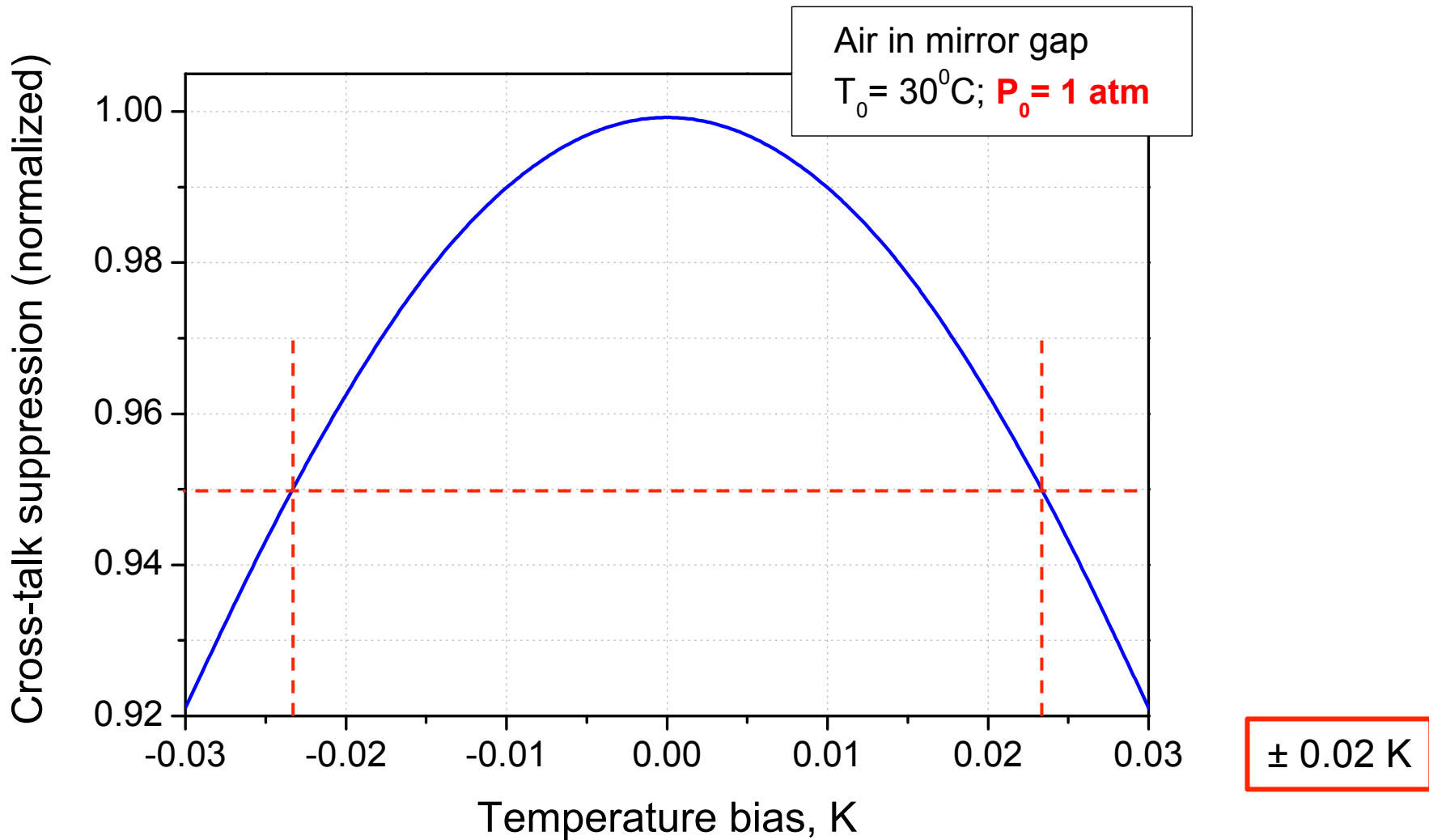
$$\Delta f_{355} = 135 \text{ MHz}; R = 0.44; d = 30 \text{ mm}$$

$$d_p = 0.2 \text{ mm}; F_L = 120 \text{ mm}; D_{\text{FPI}} = 40 \text{ mm}; F_d = 30; n = 1$$



Air temperature impact

3xFPI, 355 nm



$$\Delta f_{355} = 135 \text{ MHz}; R = 0.44; d = 30 \text{ mm}$$

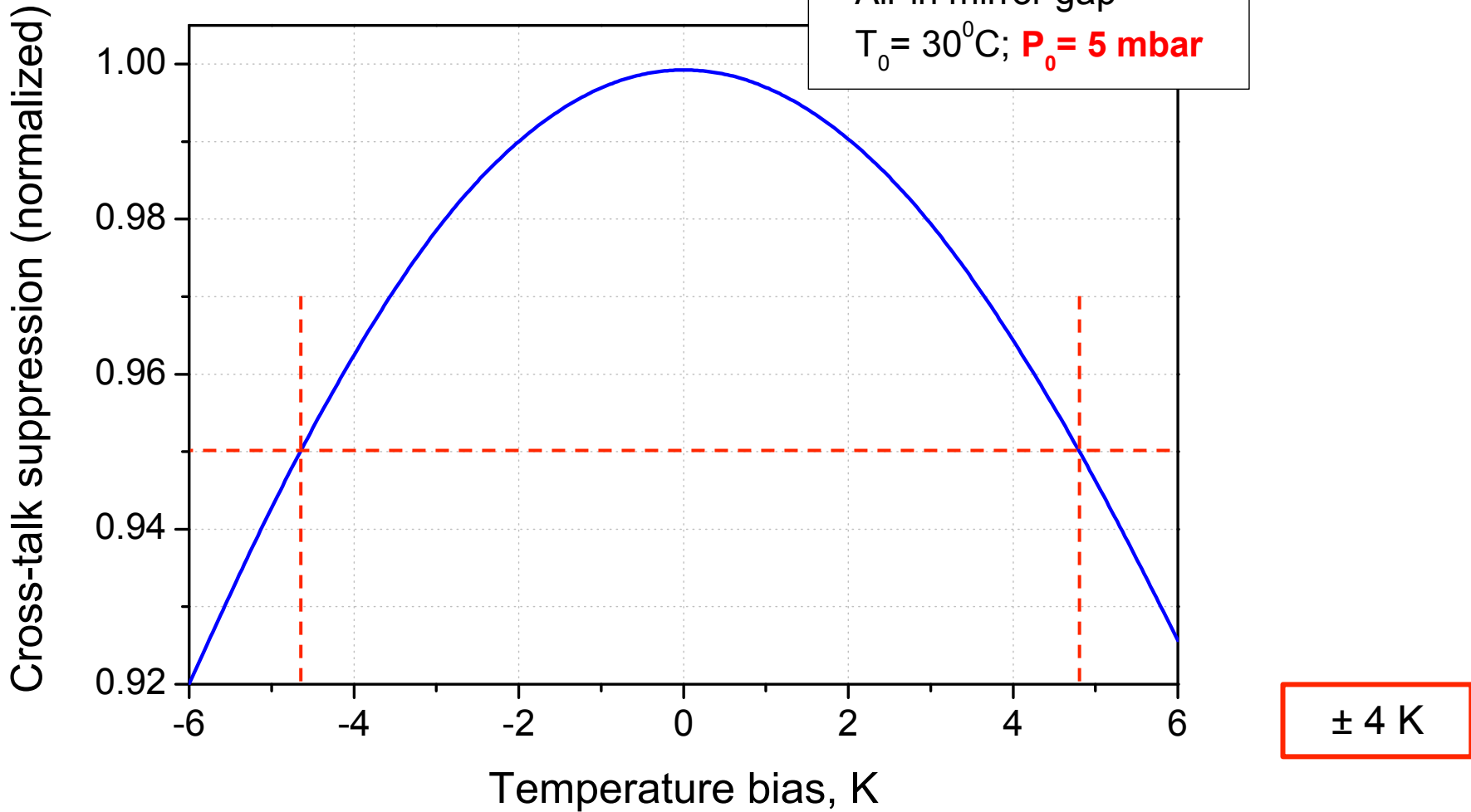
$$d_p = 0.2 \text{ mm}; F_L = 120 \text{ mm}; D_{\text{FPI}} = 40 \text{ mm}; F_d = 30$$

Air temperature impact

3xFPI, 355 nm

Air in mirror gap

$T_0 = 30^\circ\text{C}$; $P_0 = 5 \text{ mbar}$



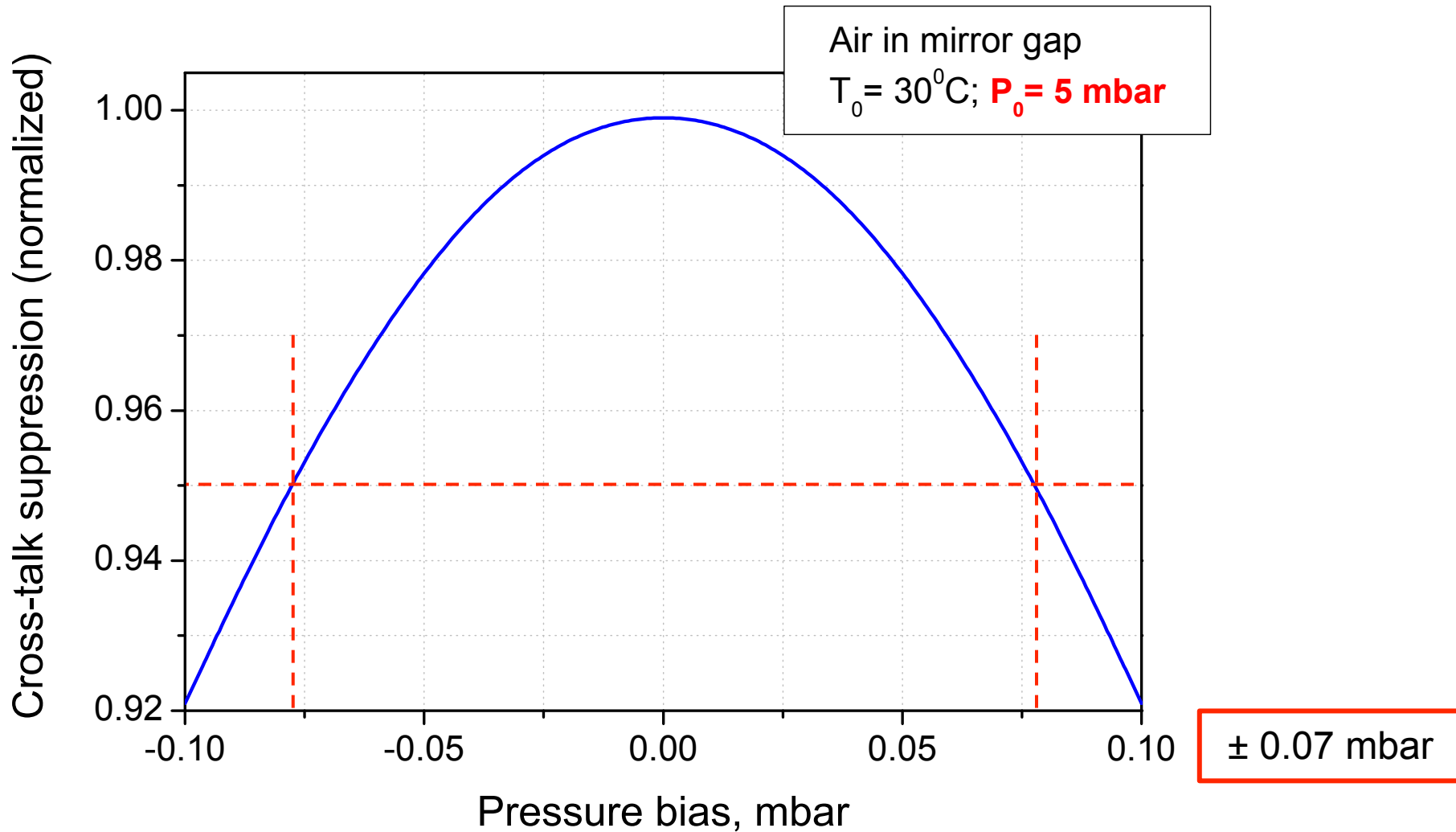
$$\Delta f_{355} = 135 \text{ MHz}; R = 0.44; d = 30 \text{ mm}$$

$$d_p = 0.2 \text{ mm}; F_L = 120 \text{ mm}; D_{\text{FPI}} = 40 \text{ mm}; F_d = 30$$



Air pressure impact

3xFPI, 355 nm

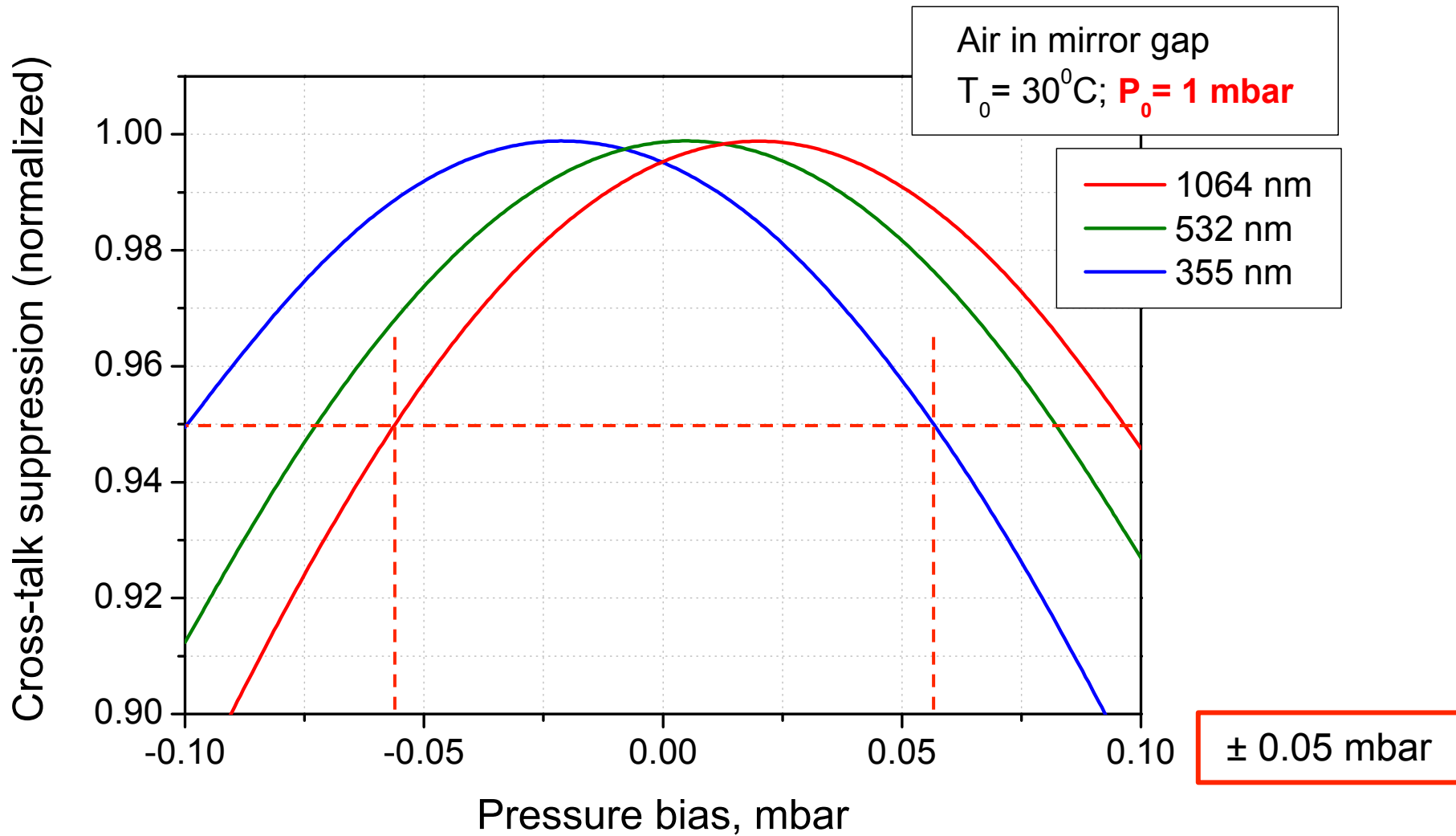


$$\Delta f_{355} = 135 \text{ MHz}; R = 0.44; d = 30 \text{ mm}$$

$$d_p = 0.2 \text{ mm}; F_L = 120 \text{ mm}; D_{\text{FPI}} = 40 \text{ mm}; F_d = 30$$

Tuning for “1064 & 532 & 355”

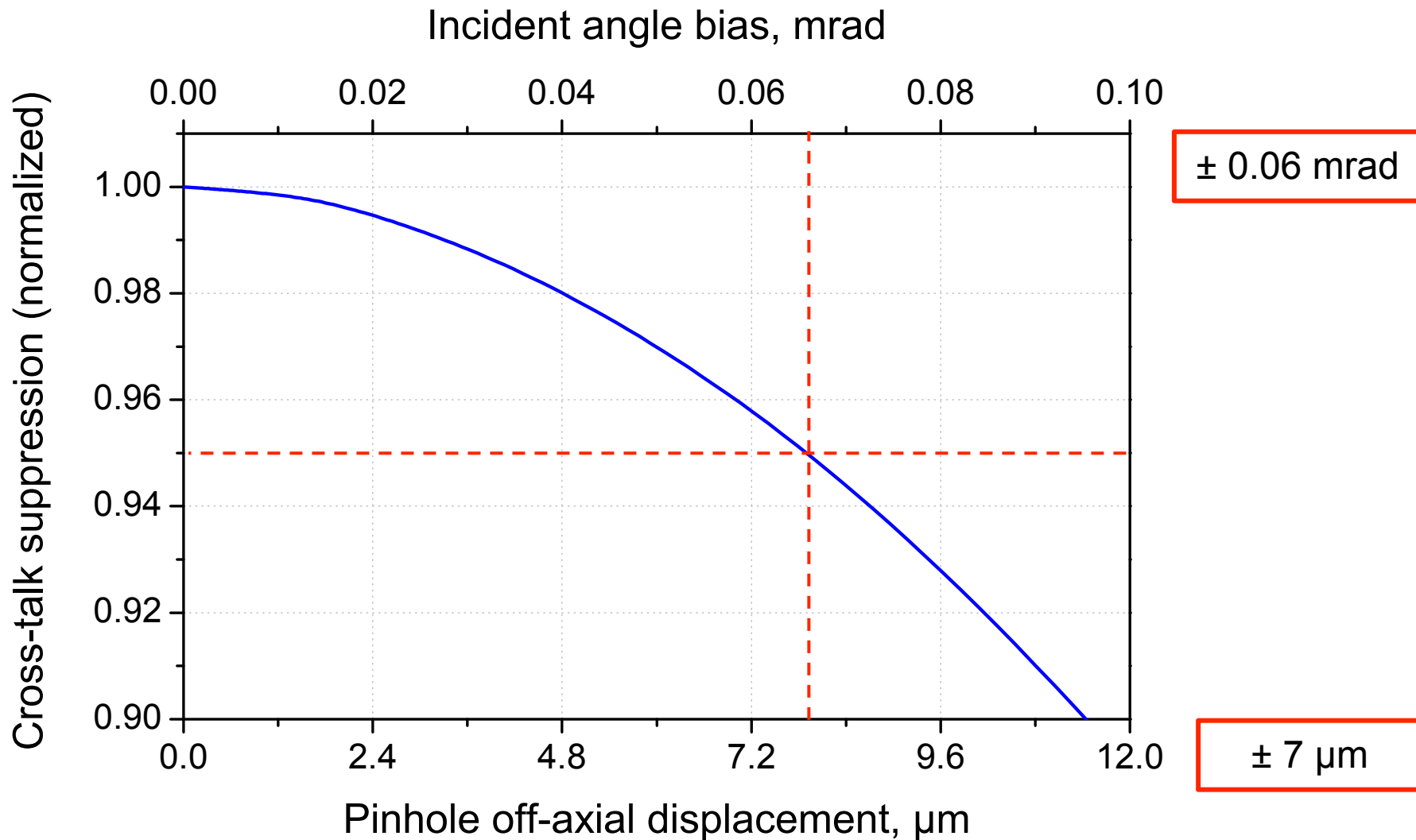
3xFPI



$$\Delta f_{1064} = 45 \text{ MHz}; \Delta f_{532} = 90 \text{ MHz}; \Delta f_{355} = 135 \text{ MHz}; R = 0.44; d = 30 \text{ mm}$$
$$d_p = 0.2 \text{ mm}; F_L = 120 \text{ mm}; D_{\text{FPI}} = 40 \text{ mm}; F_d = 30$$

Mechanical stability

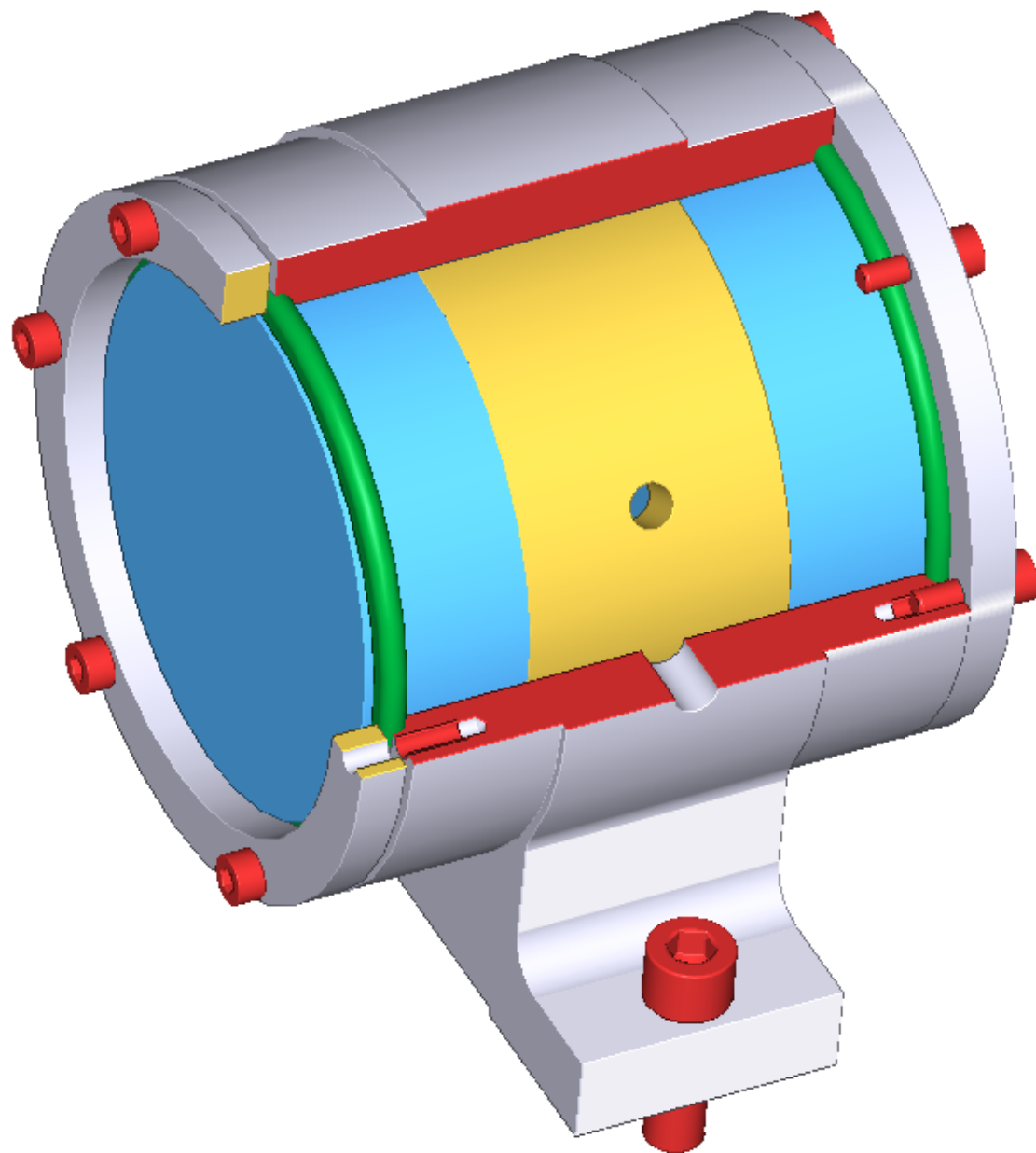
3xFPI, 355 nm



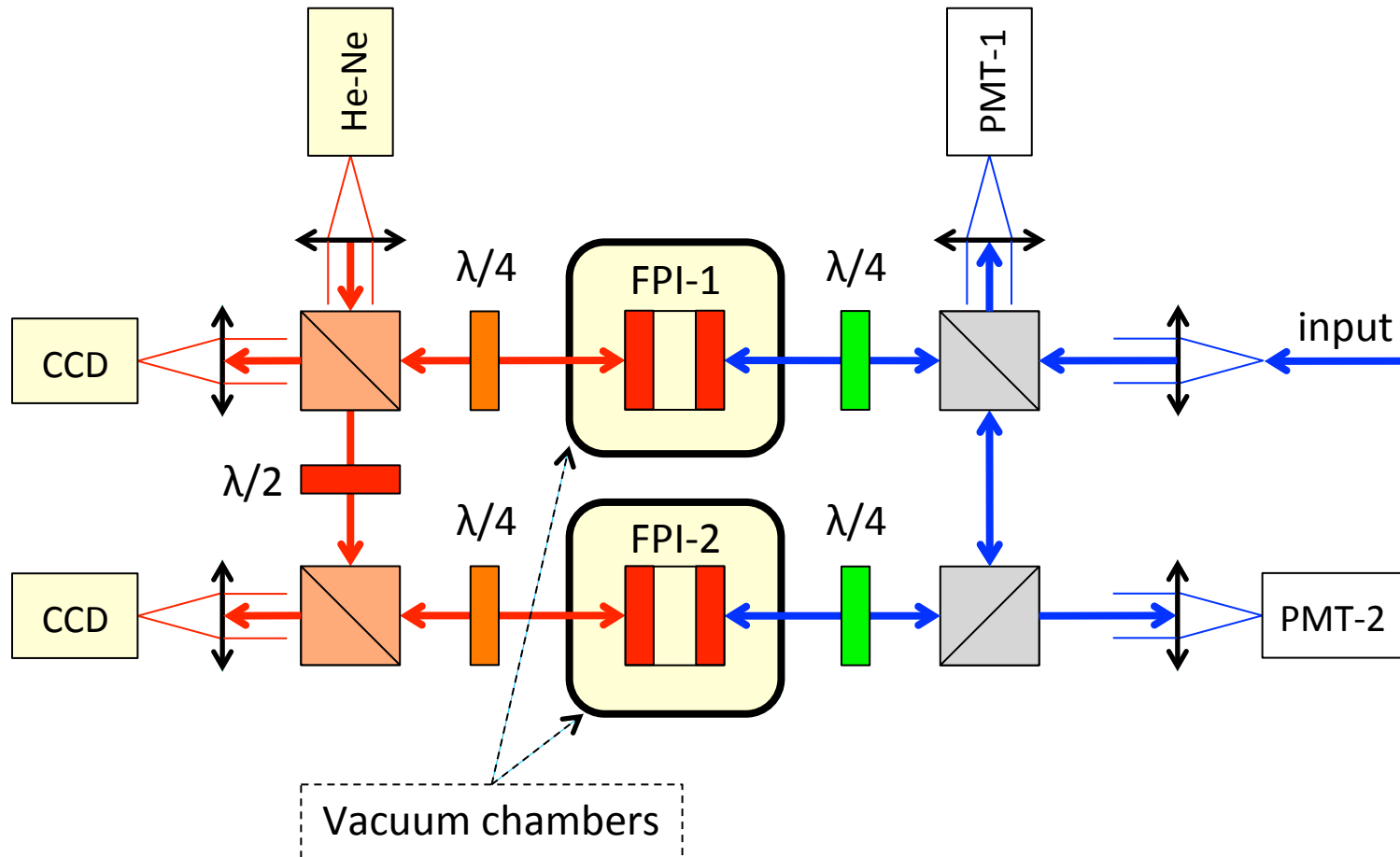
$$\Delta f_{355} = 135 \text{ MHz}; R = 0.44; d = 30 \text{ mm}$$

$$d_p = 0.2 \text{ mm}; F_L = 120 \text{ mm}; D_{\text{FPI}} = 40 \text{ mm}; F_d = 30$$

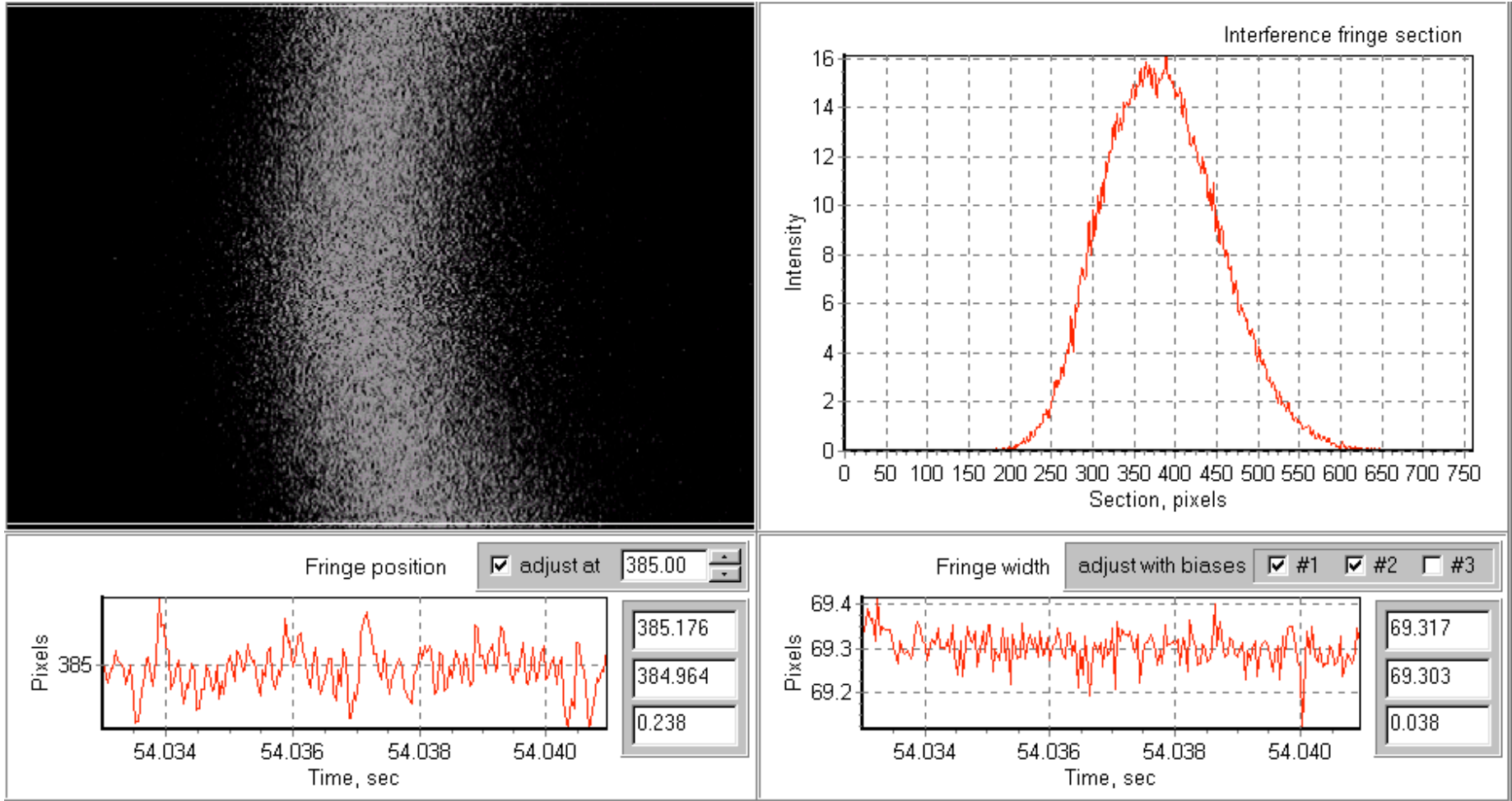




Conceptual optical layout

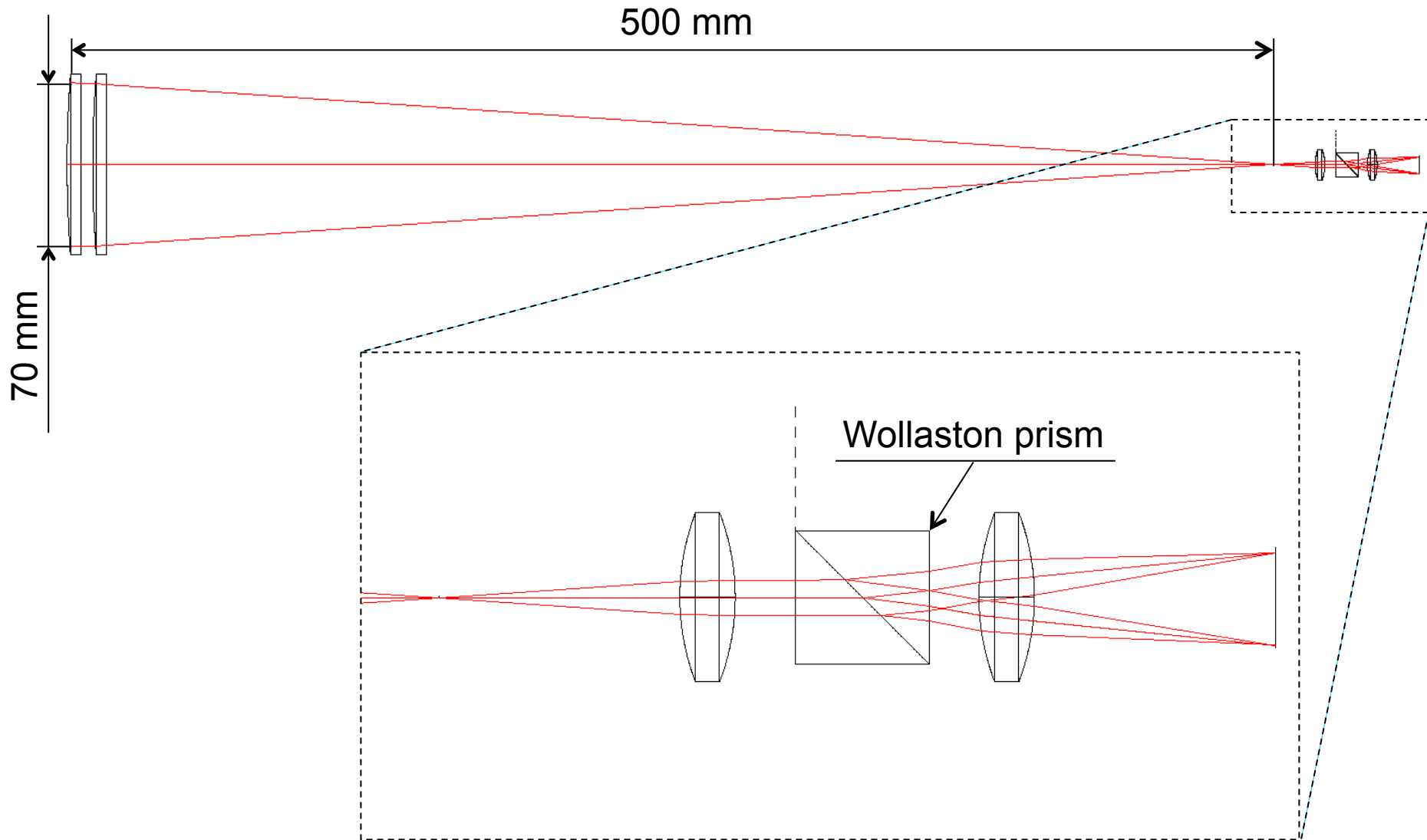


FPI alignment control by analyzing interference pattern of He-Ne light

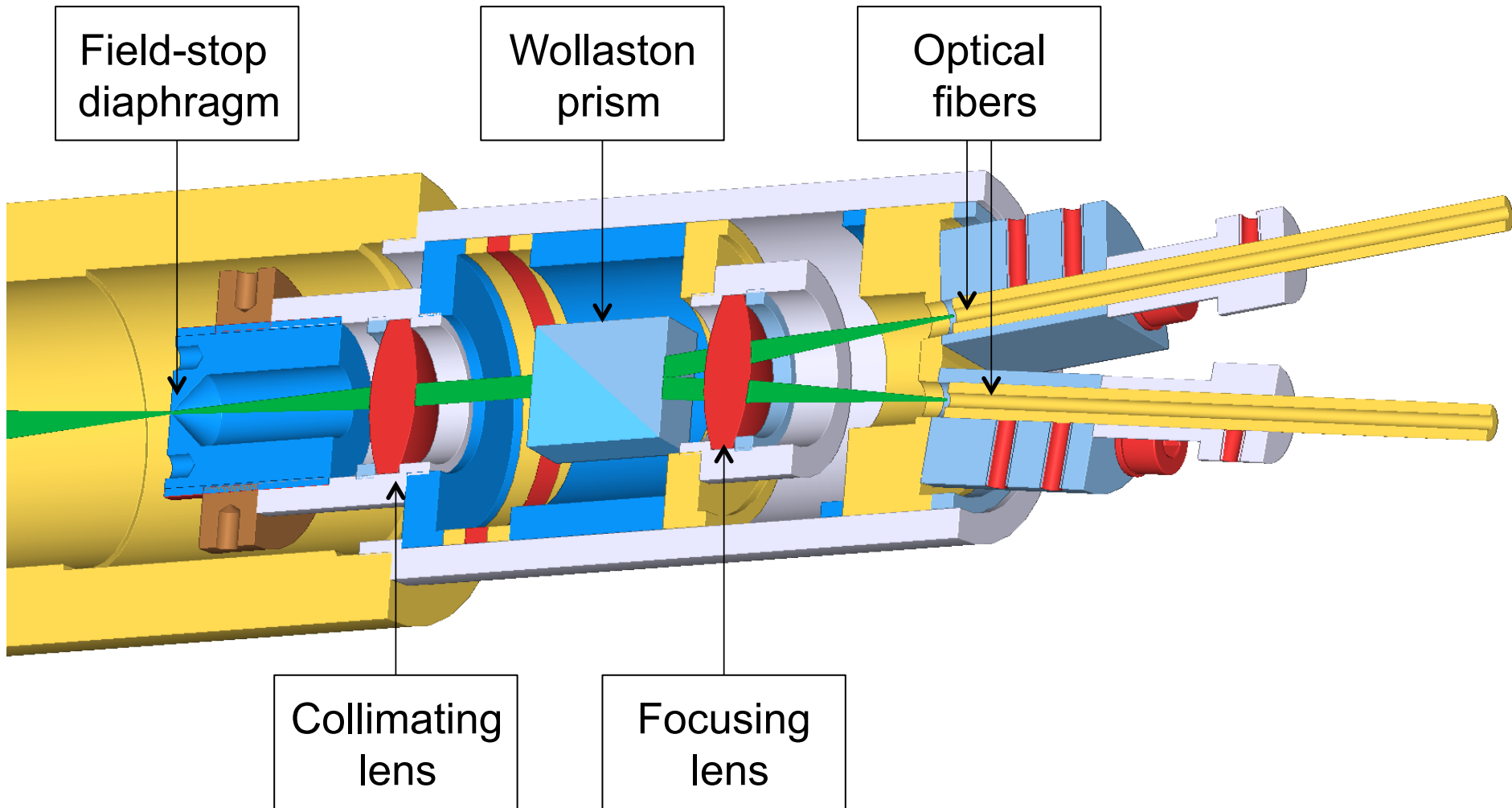


The standard deviation of fringe position (i.e. fringe radius) was measured to be about 0.24 pixel that corresponds to mirror spacing instability of 0.2 nm.

Depolarization channel, principle layout



Depolarization channel, 3D-model



Thank you!

